Copy 609

CONFIDENTIAL NASA TM X-423

NASA TM X-423

...fication changed to declassified
April

[redacted]

N65-13904

# TECHNICAL MEMORANDUM

X-423

## STATIC LONGITUDINAL AERODYNAMIC CHARACTERISTICS AT TRANSONIC SPEEDS OF A LENTICULAR-SHAPED REENTRY VEHICLE

By John P. Mugler, Jr., and Walter B. Olstad

Langley Research Center
Langley Field, Va.

[redacted]

NATIONAL AERONAUTICS AND SPACE ADMINISTRATION

WASHINGTON December 1960

CONFIDENTIAL

NATIONAL AERONAUTICS AND SPACE ADMINISTRATION

TECHNICAL MEMORANDUM X-423

# STATIC LONGITUDINAL AERODYNAMIC CHARACTERISTICS AT TRANSONIC SPEEDS OF A LENTICULAR-SHAPED REENTRY VEHICLE*

By John P. Mugler, Jr., and Walter B. Olstad

## SUMMARY

Tests have been made at transonic speeds on a lenticular-shaped reentry vehicle. The tests covered a Mach number range from 0.40 to 1.20 at angles of attack from approximately $-3^{\circ}$ to $102^{\circ}$. Tests were made on body-alone and body-fin configurations. The Reynolds number based on body length varied during the tests from about $1.2 \times 10^{6}$ to $4.4 \times 10^{6}$.

The results indicate that the body-alone configuration was statically unstable at angles of attack near $0^{\circ}$ and stable at angles of attack near $90^{\circ}$. Addition of horizontal fins with no deflection resulted in a neutrally stable configuration near $0^{\circ}$ at most Mach numbers and slightly increased the stability at angles of attack near $90^{\circ}$. At transonic speeds and moderate angles of attack separated flow was prominent on the body upper surface and caused horizontal-fin ineffectiveness at these test conditions. Deflecting the fins $-20^{\circ}$ caused the configuration to trim at a higher angle of attack at all Mach numbers. Maximum lift-drag ratios of about 5.5 were obtained on both the body-alone and body-fin configurations at $M = 0.4$, and this value diminished to about 1.0 at low-supersonic speeds.

## INTRODUCTION

At the present time the reentry requirements of space vehicles are not clearly defined, and vehicles having maximum lift-drag ratios from 0 to about 2 at hypersonic speeds are being studied. Therefore, an extensive investigation is in progress at the Langley Research Center to study the aerodynamic characteristics at subsonic to hypersonic speeds of a wide variety of generalized lifting-body shapes suitable for reentry vehicles. Since some of these vehicles may traverse a large

*Title, Unclassified.

portion of the flight path at high angles of attack, these studies generally cover a large angle range.

The present paper presents the static longitudinal aerodynamic characteristics at transonic speeds on one vehicle - a lenticular-shaped body with and without movable fins which provide longitudinal control. The tests on this lenticular-shaped vehicle were also made in support of studies currently being made by NASA Space Task Group. The tests were conducted in the Langley 8-foot transonic pressure tunnel at Mach numbers from 0.40 to 1.20 and at angles of attack up to approximately 100°. Tests on similar vehicles have been conducted at supersonic speeds and at low-subsonic speeds, and the results have been presented in references 1, 2, and 3.

## SYMBOLS

$C_A$ axial-force coefficient, $\frac{\text{Axial force}}{qS}$

$C_D$ drag coefficient, $\frac{\text{Drag}}{qS}$

$C_{D,min}$ minimum drag coefficient

$C_L$ lift coefficient, $\frac{\text{Lift}}{qS}$

$C_m$ pitching-moment coefficient, $\frac{\text{Pitching moment about c.g.}}{qSl}$
(c.g. at $0.45l$, see fig. 1)

$C_N$ normal-force coefficient, $\frac{\text{Normal force}}{qS}$

$C_{p,b}$ base-pressure coefficient, $\frac{p_b - p}{q}$

$(L/D)_{max}$ maximum lift-drag ratio

| | |
|---|---|
| $l$ | body length, in. |
| M | free-stream Mach number |
| p | free-stream static pressure, lb/sq ft |
| $p_b$ | static pressure at model base, lb/sq ft |
| q | free-stream dynamic pressure, lb/sq ft |
| R | Reynolds number based on body length |
| S | body planform area, excluding fins, sq ft |
| $\alpha$ | angle of attack, deg |
| $\delta$ | fin deflection angle, positive when trailing edge down, deg |

## APPARATUS

### Tunnel

The investigation was conducted in the Langley 8-foot transonic pressure tunnel. The test section of this facility is rectangular in cross section. The upper and lower walls are slotted longitudinally to allow continuous operation through the transonic speed range with negligible effects of choking and blockage. During this investigation the tunnel was operated at stagnation pressures from about 1/3 to 1 atmosphere. The dewpoint of the tunnel air was controlled and was kept constant at approximately $0^{\circ}$ F. The stagnation temperature of the tunnel air was automatically controlled and was kept constant at about $120^{\circ}$ F. Control of both dewpoint and stagnation temperature in this manner minimized humidity effects. Details of the test section are presented in reference 4.

### Models

Details of the lenticular-shaped model used during this investigation are shown in figure 1, and photographs of the model are presented in figure 2. The body shape was generated by revolving an ellipse, having a major-to-minor-axis ratio of 2.73, about its minor axis. The horizontal fins were flat plates with the leading edges rounded and vertical end plates on the tips. The fin deflection angle $\delta$ is the angle generated by rotating the horizontal fin about its hinge line and is positive when the trailing edge of the fin is deflected down. The end plates were rigidly attached to the horizontal fins so that the entire fin structure was deflected.

At angles of attack from about $-3^{\circ}$ to $20^{\circ}$ the model was supported in the tunnel by a conventional sting which extended from the base of the body and was, in turn, attached to the central support system of the tunnel. (See figs. 1(a) and 2(a).) A three-component internal strain-gage balance was attached to the forward end of the sting and was housed within the body. At angles of attack greater than $20^{\circ}$ an adapter was attached to the forward end of the sting and fitted into a cavity on top of the body. (See figs. 1(b) and 2(b).) The movable tongue of the adapter, which was attached to the balance, was fixed at angles from $20^{\circ}$ to $90^{\circ}$ to obtain data at the high angles of attack. When the adapter was used, a base plug was fitted into the hole at the model base provided for the low-angle sting. (See figs. 1(b) and 2(b).) These support systems kept the model near the center line of the tunnel at all angles of attack.

## TESTS

Tests were made on the body alone, body-fin combination with no fin deflection ($\delta = 0^{\circ}$), and on the body-fin combination with the fins deflected $20^{\circ}$, trailing edge up ($\delta = -20^{\circ}$). The measured fin deflection angles are as follows:

| Fin | Measured fin deflection angles, deg, for - | |
|---|---|---|
| | $\delta = 0^{\circ}$ | $\delta = -20^{\circ}$ |
| Right | -0.63 | -21.60 |
| Left | .03 | -20.87 |

The nominal deflection angles of $0^{\circ}$ and $-20^{\circ}$ will be used in the remainder of the paper.

Tests were made at Mach numbers from 0.40 to 1.20 at angles of attack from about $-3^{\circ}$ to $102^{\circ}$. At Mach numbers between 1.03 and 1.13, boundary reflected disturbances influenced the model so no data were recorded in this Mach number range.

Tests were made at stagnation pressures from about 1/3 to 1 atmosphere depending on Mach number and angle of attack. Therefore, the Reynolds number based on body length varied during the tests from about $1.2 \times 10^6$ to $4.4 \times 10^6$. (See fig. 3.) Trajectory calculations for a full-scale vehicle of this shape indicate that the flight Reynolds number based on body length for a typical reentry flight plan might vary from about $4.9 \times 10^6$ at $M = 1.2$ to $8.5 \times 10^6$ at $M = 0.6$.

All tests were made with natural transition.

## MEASUREMENTS AND ACCURACY

A study of the factors affecting the accuracy of the results indicates that the measured coefficients are accurate within the following limits:

| M | Accuracy of - | | |
|---|---|---|---|
| | $C_N$ | $C_A$ | $C_m$ |
| 0.40 | ±0.054 | ±0.0038 | ±0.0090 |
| .60 | ±.028 | ±.0019 | ±.0046 |
| 1.20 | ±.028 | ±.0019 | ±.0045 |

The angle of attack which was measured with a strain-gage attitude transmitter mounted in the tunnel central support tube was adjusted for flow angularity and balance and sting deflections under load. The angle of attack is estimated to be accurate within $\pm 0.1^{\circ}$.

Calibrations of the tunnel test section indicate that local deviations from the average free-stream Mach number are of the order of ±0.005 at subsonic speeds. With increases in Mach number, these deviations increase but do not exceed ±0.010 in the region of the model at $M = 1.20$. Several representative Mach number distributions along the center of the test section are presented in reference 4. The average free-stream Mach number was held to within ±0.005 of the nominal values shown in this paper.

The pressure in the region of the model base was measured during the tests and is presented as base-pressure coefficient in figure 4. For the low-angle tests ($\alpha = -3^\circ$ to $20^\circ$) the base-pressure tube was mounted on the sting several inches forward of the model base. For the high-angle tests ($\alpha = 20^\circ$ to $102^\circ$) the base-pressure tube was located near the bottom of the cavity provided for the knuckle. It is estimated that the accuracy of these base-pressure coefficients is within ±0.010.

## CORRECTIONS

No corrections have been applied to the data for boundary-interference effects. At subsonic speeds, the slotted test section minimized boundary-interference effects such as blockage and boundary-induced upwash.

The effects of the presence of the high-angle knuckle were not determined during these tests, and no corrections have been applied to the data to account for support interference. The axial and drag data presented have not been adjusted to free-stream conditions at the model base.

## RESULTS

The aerodynamic coefficients plotted against angle of attack for the three configurations tested are presented in figure 5. These coefficients are also tabulated in tables I, II, and III along with the base-pressure coefficients. At a Mach number of 0.80 no data were obtained at angles of attack below about $20^\circ$ for the body-alone configuration. For the body-fin, $\delta = -20^\circ$ configuration the highest test angle of attack was about $73^\circ$. As was noted previously, the high-angle adapter was installed near $20^\circ$ to obtain data at high angles of attack. Data at angles of attack of approximately $20^\circ$ were also obtained using the low-angle sting. (See tables I to III.) In most cases the data obtained using both support systems agreed reasonably well; however, in some instances the agreement was poor. Therefore, the fairings of the curves in figure 5 in the region of $20^\circ$ are rather arbitrary. Figure 6 presents schlieren photographs taken during the tests of the body-alone configuration at an angle of attack of approximately $20^\circ$. Figures 7, 8, 9, and 10 present analysis curves. The slopes in figure 7 were taken at angles of attack between $-3^\circ$ and $4^\circ$. The slopes in figure 9 were taken at angles of attack between $82^\circ$ and $102^\circ$. The other quantities in figures 7 to 10 were obtained from the faired curves.

## DISCUSSION

### Body-Alone Configuration

The aerodynamic characteristics for the body-alone configuration shown in figure 5 show that the lift curve has a positive slope up to an angle of attack of about 30° or 40° (maximum lift) and a negative slope over the remainder of the angle range tested. As would be expected, the drag coefficients reach a maximum around an angle of attack of 90°. The pitching-moment-coefficient curves (c.g. at 45 percent of the body length) have a positive slope up to about the angle of attack for maximum lift and then a negative slope over the remainder of the angle range. The normal-force coefficients appear to be reaching a maximum value at angles of attack near 100°. At Mach numbers of 0.80 and above, the axial-force coefficients generally decrease with increasing angle of attack from a positive value at -3° to 0 at an angle of attack of approximately 90°. At a Mach number of 0.60, negative values of the axial-force coefficient were obtained at angles of attack near 30°, probably because of leading-edge thrust developed by this configuration.

The schlieren photographs at $\alpha \approx 20^{\circ}$ for the body-alone configuration presented in figure 6 show that at Mach numbers of 0.80 and 0.95 a large separated wedge is formed on the body upper surface. With increases in Mach number this separated region diminishes in thickness and extent. At Mach numbers of 1.13 and 1.20 the strong shock indicated by the broad white line is the model bow wave striking the tunnel wall.

The lift-curve slope at angles of attack near 0° (fig. 7(a)) for the body-alone configuration was about 0.01 at the low Mach numbers and increased at transonic speeds to a value of about 0.022. The moment characteristics at angles of attack near 0° (fig. 7(b)) indicate that the body-alone configuration is statically unstable throughout the entire Mach number range tested. The minimum-drag curve (fig. 7(c)) exhibits typical drag-rise characteristics at transonic speeds. The maximum lift-drag-ratio characteristics (fig. 8) show that a maximum lift-drag ratio of about 5.5 was obtained at $M = 0.4$. With increases in Mach number, the maximum lift-drag ratio decreased rapidly to about $M = 0.90$ where it leveled out at a value of about 1.0. The lift coefficient for maximum lift-drag ratio increased with increases in Mach number from about 0.04 at $M = 0.4$ to about 0.44 at $M = 1.2$. The angle of attack for maximum lift-drag ratio increased with increases in Mach number from about 4° at $M = 0.4$ to 20° at $M = 1.2$.

At angles of attack near 90° the lift-curve slope for the body-alone configuration has a negative value of about -0.011 at Mach numbers from 0.6 to 0.8 (fig. 9(a)). Further increases in Mach number cause the lift-curve slope to increase negatively to a value of about -0.016 at a Mach number of 1.2. The slope of the pitching-moment curves at angles of attack near $90^{\circ}$ for the body-alone configuration (fig. 9(b)) is constant through the Mach number range tested and indicates that the body alone is statically stable. The drag coefficient at an angle of attack of $90^{\circ}$ gradually increases with increases in Mach number up to a Mach number of about 1.1 and did not exhibit the pronounced drag-rise characteristics noted at an angle of attack of $0^{\circ}$.

In reference 5 it was pointed out that for flat wings a good approximation of the lift-curve slope (per radian) at an angle of attack of $90^{\circ}$ was the negative of the drag coefficient at an angle of attack of $90^{\circ}$; therefore,

$$\left(\frac{\partial C_L}{\partial \alpha}\right)_{\alpha=90^{\circ}} \approx -C_{D,\alpha=90^{\circ}} \tag{1}$$

The basis for this approximation can be seen by noting that

$$C_L = C_N \cos \alpha - C_A \sin \alpha \tag{2}$$

then

$$\frac{\partial C_L}{\partial \alpha} = -\left(C_N + \frac{\partial C_A}{\partial \alpha}\right)\sin \alpha + \left(\frac{\partial C_N}{\partial \alpha} - C_A\right)\cos \alpha \tag{3}$$

and at an angle of attack of $90^{\circ}$

$$\left(\frac{\partial C_L}{\partial \alpha}\right)_{\alpha=90^{\circ}} = -C_{N,\alpha=90^{\circ}} - \left(\frac{\partial C_A}{\partial \alpha}\right)_{\alpha=90^{\circ}} \tag{4}$$

but

$$C_D = C_A \cos \alpha + C_N \sin \alpha \tag{5}$$

and at an angle of attack of $90^{\circ}$

$$C_{D,\alpha=90^{\circ}} = \left(C_N\right)_{\alpha=90^{\circ}} \tag{6}$$

therefore

$$\left(\frac{\partial C_L}{\partial \alpha}\right)_{\alpha=90^\circ} = -C_{D,\alpha=90^\circ} - \left(\frac{\partial C_A}{\partial \alpha}\right)_{\alpha=90^\circ} \tag{7}$$

It was noted in reference 5 that the value of $\left(\frac{\partial C_A}{\partial \alpha}\right)$ was small for flat wings, generally less than 2 percent of the value of the drag coefficient at $90^\circ$, and can therefore be neglected to give equation (1). It is of interest to note that for the present configuration this approximation is not valid. Figures 9(c) and (d) show that the contribution of $\left(\frac{\partial C_A}{\partial \alpha}\right)_{\alpha\approx 90^\circ}$ is of the order of 25 percent of $C_{D,\alpha=90^\circ}$ and neglecting it would result in values of $\left(\frac{\partial C_L}{\partial \alpha}\right)_{\alpha\approx 90^\circ}$ which were of the order of 30 percent too high.

## Body-Fin, $\delta = 0^\circ$ Configuration

The effects on the basic aerodynamic characteristics of adding the horizontal fin to the body-alone configuration can be seen in figure 5. The addition of the fin generally caused the angle of attack at which maximum lift occurred to increase, caused the drag coefficient to increase at all test conditions, and caused marked changes in the pitching-moment characteristics. An interesting effect is evident at Mach numbers of 0.90 and 0.95 at angles of attack from about $-3^\circ$ to $20^\circ$. At these test conditions the addition of the horizontal fin caused little or no change in the lift- and pitching-moment-coefficient characteristics. The schlieren photographs previously noted for the body-alone configuration (fig. 6) indicate that a large portion of the horizontal fins may have been blanketed by the separated upper-surface flow and thus were ineffective. The schlieren photographs indicate that this condition is gradually diminished with increases in Mach number and the lift- and pitching-moment-coefficient data in figures 5(a) and (c), respectively, are consistent with this premise.

At low angles of attack the addition of the horizontal fin caused large increases in the lift-curve slope up to a Mach number of about 0.8 and some increases above $M = 1.0$ (fig. 7(a)). Even though the addition of the fin decreased the slope of the pitching-moment-coefficient curve at all Mach numbers at $\alpha \approx 0^\circ$, the body-fin, $\delta = 0^\circ$ configuration was still unstable or neutrally stable at all Mach numbers below about 1.0 (fig. 7(b)). The minimum drag coefficient for the body-fin, $\delta = 0^\circ$ configuration was generally increased slightly over the body-alone values (fig. 7(c)).

The maximum lift-drag-ratio characteristics (fig. 8) indicate that the addition of the fin produced little or no change in the maximum lift-drag ratio. The addition of the fin was responsible for some increases in the lift coefficient and angle of attack for maximum lift-drag ratio.

At angles of attack near $90^\circ$ the addition of the fin caused an increase in the negative lift-curve slope, a slight increase in the negative pitching-moment-curve slope, and a rather large increase in the drag coefficient (fig. 9).

### Body-Fin, $\delta = -20^\circ$ Configuration

The effects of deflecting the fin $-20^\circ$ (trailing edge up) on the basic aerodynamic characteristics can be seen in figure 5. The ineffectiveness of the fins to produce lift and pitch increments at Mach numbers of 0.90 and 0.95 at moderate angles of attack is evident for the $\delta = -20^\circ$ fin configuration as it was for the $\delta = 0^\circ$ configuration. (See figs. 5(a) and (c).) However, the angle-of-attack range over which this ineffectiveness occurred was reduced to about $7\frac{1}{2}^\circ$ to $20^\circ$ for the $\delta = -20^\circ$ fin configuration as compared to about $-3^\circ$ to $20^\circ$ for the $\delta = 0^\circ$ fin configuration. As would be expected, the body-fin, $\delta = -20^\circ$ configuration trimmed at a higher angle of attack at all Mach numbers than the $\delta = 0^\circ$ configuration (fig. 5(c)). It is likely that the model could be trimmed at intermediate angles of attack by using suitable fin deflections between $0^\circ$ and $-20^\circ$. The incremental pitching-moment coefficients due to a fin deflection of $-20^\circ$ are plotted against the angle of attack in figure 10. At Mach numbers above 0.60, these incremental pitching-moment coefficients exhibited a minimum value at angles of attack around $15^\circ$ to $25^\circ$ and at Mach numbers of 0.90 and 0.95, the value dropped to about 0 at an angle of attack of approximately $15^\circ$. This reduction in the pitching-moment-coefficient increment is a result of the separated flow prevalent on the body upper surface that was noted previously.

## CONCLUSIONS

Analysis of data from tests at transonic speeds on a lenticular-shaped reentry vehicle has led to the following conclusions:

1. The body-alone configuration was statically unstable at angles of attack near $0^\circ$ but was stable at angles of attack near $90^\circ$. Maximum lift-drag ratios of about 5.5 were obtained for the body-alone configuration at a Mach number of 0.4 but diminished to about 1.0 at low-supersonic speeds.

2. The addition of horizontal fins with no deflection decreased the slope of the pitching-moment-coefficient curves at angles of attack near $0^{\circ}$, but this configuration was still neutrally stable or unstable over most of the Mach number range. At angles of attack near $90^{\circ}$ the addition of the fins resulted in slightly increased stability over the Mach number range. The addition of fins had little or no effect on the maximum lift-drag ratio.

3. At transonic speeds and moderate angles of attack, separated flow was prevalent on the body upper surface. As a result of this, the fins were not effective at these test conditions.

4. Deflecting the fins $-20^{\circ}$ caused the configuration to trim at a higher angle of attack at all Mach numbers.

Langley Research Center,
National Aeronautics and Space Administration,
Langley Field, Va., September 1, 1960.

REFERENCES

1. Jackson, Charlie M., Jr., and Harris, Roy V., Jr.: Static Longitudinal Stability and Control Characteristics at a Mach Number of 1.99 of a Lenticular-Shaped Reentry Vehicle. NASA TN D-514, 1960.

2. Letko, William: Experimental Investigation at a Mach Number of 3.11 of the Lift, Drag, and Pitching-Moment Characteristics of Five Blunt Lifting Bodies. NASA TN D-226, 1960.

3. Ware, George M.: Static Stability and Control Characteristics at Low-Subsonic Speeds of a Lenticular Reentry Configuration. NASA TM X-431, 1960.

4. Mugler, John P., Jr.: Transonic Wind-Tunnel Investigation of the Aerodynamic Loading Characteristics of a 60° Delta Wing in the Presence of a Body With and Without Indentation. NACA RM L55G11, 1955.

5. Phillips, William H.: Research on Blunt-Faced Entry Configurations at Angles of Attack Between 60° and 90°. NASA TM X-315, 1960.

TABLE I.- AERODYNAMIC COEFFICIENTS FOR BODY-ALONE CONFIGURATION

| Support | α, deg | $C_L$ | $C_D$ | $C_m$ | $C_N$ | $C_A$ | $C_{p,b}$ |
|---|---|---|---|---|---|---|---|
| | | | | M = 0.40 | | | |
| Low-angle sting | -3.0 | -0.022 | 0.0039 | -0.0300 | -0.022 | 0.0027 | 0.3339 |
| | .0 | .019 | .0040 | -.0051 | .019 | .0040 | .3626 |
| | .0 | .019 | .0040 | -.0037 | .019 | .0040 | .3625 |
| | .0 | .000 | .0009 | .0010 | .000 | .0009 | .0000 |
| | 4.0 | .042 | .0057 | .0382 | .042 | .0027 | .3555 |
| | 8.1 | .082 | .0144 | .0733 | .083 | .0027 | .3125 |
| | 12.1 | .140 | .0277 | .1047 | .143 | -.0024 | .2550 |
| | 16.2 | .196 | .0501 | .1302 | .202 | -.0064 | .1904 |
| | 20.2 | .279 | .0780 | .1501 | .289 | -.0230 | .1658 |
| | | | | M = 0.60 | | | |
| Low-angle sting | -3.0 | -0.008 | 0.0152 | -0.0333 | -0.009 | 0.0147 | 0.2749 |
| | .0 | .028 | .0150 | -.0064 | .028 | .0150 | .2907 |
| | .0 | .051 | .0157 | -.0104 | .051 | .0157 | .2934 |
| | 4.1 | .070 | .0161 | .0338 | .071 | .0111 | .3027 |
| | 8.2 | .120 | .0271 | .0704 | .122 | .0095 | .2450 |
| | 12.2 | .155 | .0359 | .1077 | .159 | .0052 | .1904 |
| | 16.3 | .218 | .0548 | .1386 | .225 | -.0086 | .1713 |
| | 20.4 | .298 | .0827 | .1615 | .308 | -.0285 | .1405 |
| High-angle adapter | 20.5 | .222 | .0730 | .1593 | .235 | -.0047 | .1351 |
| | 20.5 | .228 | .0802 | .1589 | .242 | -.0049 | .1354 |
| | 31.0 | .556 | .2030 | .1907 | .543 | -.1076 | .0950 |
| | 41.0 | .465 | .4709 | .1226 | .660 | .0506 | -.4117 |
| | 50.9 | .331 | .5344 | .0927 | .623 | .0802 | -.4180 |
| | 50.9 | .334 | .5395 | .0925 | .629 | .0809 | -.4179 |
| | 60.9 | .229 | .6230 | .0649 | .660 | .1049 | -.3876 |
| | 70.9 | .140 | .7054 | .0320 | .713 | .0980 | -.3780 |
| | 80.9 | .080 | .7641 | -.0069 | .767 | .0415 | -.3625 |
| | 80.9 | .072 | .7655 | -.0059 | .757 | .0493 | -.3597 |
| | 90.9 | -.020 | .8161 | -.0421 | .816 | .0072 | -.3506 |
| | 100.9 | -.137 | .8303 | -.0763 | .841 | -.0230 | -.4362 |
| | | | | M = 0.80 | | | |
| Low-angle sting | No low-angle data obtained | | | | | | |
| High-angle adapter | 21.1 | 0.386 | 0.2163 | 0.1216 | 0.437 | 0.0633 | -0.1924 |
| | 21.1 | .396 | .2269 | .1182 | .451 | .0691 | -.2469 |
| | 21.1 | .389 | .2183 | .1227 | .442 | .0637 | -.1865 |
| | 31.3 | .438 | .4104 | .1130 | .588 | .1229 | -.4353 |
| | 41.4 | .381 | .5447 | .0921 | .646 | .1573 | -.4724 |
| | 51.5 | .360 | .6707 | .0710 | .749 | .1352 | -.4688 |
| | 51.5 | .360 | .6687 | .0711 | .747 | .1347 | -.4655 |
| | 61.6 | .280 | .7592 | .0484 | .801 | .1150 | -.4070 |
| | 71.6 | .173 | .8188 | .0207 | .831 | .0952 | -.3696 |
| | 81.5 | .067 | .8630 | -.0106 | .863 | .0610 | -.3510 |
| | 81.5 | .066 | .8588 | -.0107 | .859 | .0610 | -.3501 |
| | 91.5 | -.039 | .9123 | -.0482 | .913 | .0141 | -.3859 |
| | 101.5 | -.140 | .9148 | -.0832 | .924 | -.0455 | -.4135 |
| | | | | M = 0.90 | | | |
| Low-angle sting | -3.1 | -0.088 | 0.1729 | -0.0118 | -0.097 | 0.1679 | -0.2359 |
| | .0 | -.039 | .1727 | .0059 | -.039 | .1727 | -.2409 |
| | 4.1 | .062 | .1796 | .0241 | .075 | .1747 | -.2423 |
| | 8.1 | .136 | .1895 | .0442 | .161 | .1694 | -.2316 |
| | 12.2 | .227 | .2229 | .0580 | .269 | .1698 | -.2702 |
| | 16.3 | .262 | .2629 | .0677 | .325 | .1790 | -.2908 |
| | 20.3 | .283 | .3141 | .0707 | .375 | .1962 | -.3435 |
| High-angle adapter | 20.9 | .353 | .3181 | .0916 | .443 | .1717 | -.3991 |
| | 20.9 | .355 | .3202 | .0927 | .446 | .1728 | -.3934 |
| | 31.1 | .388 | .4623 | .0901 | .571 | .1959 | -.4768 |
| | 41.2 | .409 | .6081 | .0737 | .708 | .1876 | -.4952 |
| | 51.6 | .394 | .7510 | .0606 | .833 | .1574 | -.4859 |
| | 51.6 | .391 | .7454 | .0602 | .827 | .1565 | -.4793 |
| | 61.7 | .323 | .8609 | .0371 | .911 | .1236 | -.4356 |
| | 71.7 | .212 | .9205 | .0103 | .940 | .0878 | -.3848 |
| | 81.9 | .083 | .9525 | -.0170 | .955 | .0515 | -.3533 |
| | 81.9 | .084 | .9542 | -.0171 | .957 | .0503 | -.3541 |
| | 91.9 | -.042 | .9929 | -.0528 | .994 | .0090 | -.3782 |
| | 101.9 | -.167 | 1.0037 | -.0857 | 1.017 | -.0429 | -.4224 |
| | | | | M = 0.95 | | | |
| Low-angle sting | -3.1 | -0.092 | 0.2186 | -0.0125 | -0.103 | 0.2133 | -0.3329 |
| | -3.1 | -.083 | .1640 | -.0112 | -.092 | .1593 | -.2237 |
| | .0 | -.032 | .1624 | .0054 | -.032 | .1624 | -.2295 |
| | .0 | -.017 | .2118 | .0016 | -.017 | .2118 | -.3191 |
| | .0 | -.022 | .2122 | .0009 | -.022 | .2122 | -.3164 |
| | 4.1 | .067 | .2133 | .0226 | .082 | .2080 | -.3152 |
| | 8.2 | .144 | .2260 | .0419 | .174 | .2033 | -.2976 |
| | 12.3 | .241 | .2677 | .0553 | .293 | .2103 | -.3610 |
| | 16.3 | .284 | .3034 | .0643 | .358 | .2114 | -.3755 |
| | 20.4 | .361 | .3775 | .0720 | .470 | .2279 | -.4487 |
| High-angle adapter | 20.8 | .375 | .3713 | .0845 | .483 | .2137 | -.4651 |
| | 20.8 | .384 | .3732 | .0838 | .491 | .2125 | -.4653 |
| | 31.0 | .407 | .4940 | .0751 | .603 | .2145 | -.5259 |
| | 41.2 | .445 | .6439 | .0665 | .759 | .1919 | -.5045 |
| | 51.6 | .441 | .8312 | .0542 | .925 | .1703 | -.5344 |
| | 51.7 | .449 | .8432 | .0536 | .940 | .1712 | -.5438 |
| | 61.7 | .357 | .9339 | .0313 | .992 | .1285 | -.4618 |
| | 71.7 | .235 | .9941 | .0040 | 1.017 | .0899 | -.4080 |
| | 81.9 | .095 | 1.0062 | -.0213 | 1.010 | .0479 | -.3622 |
| | 81.9 | .096 | 1.0096 | -.0209 | 1.013 | .0476 | -.3655 |
| | 91.9 | -.045 | 1.0565 | -.0579 | 1.057 | .0102 | -.4039 |
| | 101.9 | -.178 | 1.0587 | -.0878 | 1.073 | -.0439 | -.4291 |
| | | | | M = 1.00 | | | |
| Low-angle sting | -3.1 | -0.090 | 0.2579 | -0.0123 | -0.103 | 0.2527 | -0.3445 |
| | .0 | -.016 | .2488 | .0015 | -.016 | .2488 | -.3307 |
| | .0 | -.016 | .2500 | .0015 | -.016 | .2500 | -.3305 |
| | 4.1 | .075 | .2530 | .0184 | .093 | .2470 | -.3411 |
| | 8.2 | .179 | .2603 | .0351 | .217 | .2420 | -.3728 |
| | 12.3 | .274 | .3205 | .0505 | .335 | .2547 | -.4080 |
| | 16.4 | .347 | .3582 | .0631 | .434 | .2457 | -.4374 |
| | 20.5 | .399 | .4049 | .0702 | .512 | .2414 | -.4449 |
| High-angle adapter | 20.8 | .435 | .4411 | .0791 | .564 | .2579 | -.5088 |
| | 20.8 | .446 | .4455 | .0790 | .575 | .2581 | -.5119 |
| | 31.0 | .507 | .5894 | .0740 | .738 | .2444 | -.6422 |
| | 41.1 | .521 | .7304 | .0540 | .873 | .2075 | -.5835 |
| | 51.6 | .473 | .8733 | .0486 | .978 | .1727 | -.5442 |
| | 51.6 | .470 | .8692 | .0490 | .973 | .1722 | -.5435 |
| | 61.6 | .356 | .9937 | .0263 | 1.048 | .1324 | -.4935 |
| | 71.7 | .266 | 1.0742 | .0005 | 1.103 | .0860 | -.4505 |
| | 81.9 | .107 | 1.0681 | -.0242 | 1.073 | .0449 | -.3920 |
| | 81.9 | .107 | 1.0774 | -.0250 | 1.082 | .0458 | -.3931 |
| | 91.9 | -.044 | 1.1028 | -.0595 | 1.104 | .0089 | -.4174 |
| | 101.8 | -.190 | 1.1131 | -.0900 | 1.128 | -.0423 | -.4523 |
| | | | | M = 1.03 | | | |
| Low-angle sting | -3.1 | -0.087 | 0.2701 | -0.0120 | -0.101 | 0.2651 | -0.3386 |
| | .0 | -.020 | .2628 | .0017 | -.020 | .2628 | -.3269 |
| | .0 | -.015 | .2632 | .0023 | -.015 | .2632 | -.3257 |
| | 4.1 | .077 | .2692 | .0186 | .096 | .2631 | -.3524 |
| | 8.2 | .181 | .2962 | .0343 | .222 | .2673 | -.3962 |
| | 12.3 | .282 | .3383 | .0485 | .348 | .2703 | -.4292 |
| | 16.4 | .370 | .3850 | .0592 | .464 | .2647 | -.4576 |
| | 20.5 | .436 | .4437 | .0689 | .564 | .2627 | -.5494 |
| High-angle adapter | 20.8 | .438 | .4449 | .0751 | .567 | .2607 | -.4530 |
| | 20.8 | .446 | .4477 | .0757 | .576 | .2603 | -.4561 |
| | 31.0 | .507 | .5871 | .0726 | .737 | .2427 | -.6160 |
| | 41.1 | .519 | .7276 | .0623 | .869 | .2074 | -.5672 |
| | 51.6 | .490 | .8995 | .0466 | 1.009 | .1742 | -.5417 |
| | 51.6 | .486 | .8942 | .0468 | 1.003 | .1737 | -.5450 |
| | 61.7 | .400 | 1.0235 | .0242 | 1.091 | .1327 | -.4950 |
| | 71.7 | .273 | 1.1026 | -.0017 | 1.133 | .0564 | -.4577 |
| | 82.0 | .112 | 1.1090 | -.0260 | 1.114 | .0435 | -.4071 |
| | 82.0 | .110 | 1.1034 | -.0263 | 1.108 | .0446 | -.4073 |
| | 92.0 | -.050 | 1.1424 | -.0625 | 1.142 | .0102 | -.4324 |
| | 102.0 | -.201 | 1.1556 | -.0922 | 1.172 | -.0488 | -.4651 |
| | | | | M = 1.13 | | | |
| Low-angle sting | -3.1 | -0.082 | 0.2559 | -0.0114 | -0.095 | 0.2512 | -0.2149 |
| | .0 | -.021 | .2473 | .0018 | -.021 | .2473 | -.2017 |
| | .0 | -.021 | .2469 | .0009 | -.021 | .2469 | -.2036 |
| | 4.1 | .067 | .2495 | .0175 | .085 | .2441 | -.2303 |
| | 8.2 | .157 | .2754 | .0324 | .194 | .2502 | -.2637 |
| | 12.3 | .256 | .3192 | .0448 | .320 | .2571 | -.3011 |
| | 16.4 | .336 | .3662 | .0554 | .426 | .2560 | -.3296 |
| | 20.5 | .425 | .4360 | .0628 | .551 | .2597 | -.4118 |
| High-angle adapter | 20.8 | .404 | .4182 | .0713 | .526 | .2479 | -.3674 |
| | 20.8 | .413 | .4223 | .0705 | .536 | .2485 | -.3657 |
| | 31.0 | .501 | .5748 | .0680 | .725 | .2349 | -.4789 |
| | 41.2 | .528 | .7346 | .0586 | .881 | .2055 | -.4623 |
| | 51.5 | .483 | .8763 | .0424 | .987 | .1681 | -.4325 |
| | 51.5 | .484 | .8774 | .0428 | .988 | .1681 | -.4328 |
| | 61.5 | .393 | .9875 | .0211 | 1.055 | .1259 | -.3705 |
| | 71.6 | .277 | 1.0935 | -.0035 | 1.125 | .0833 | -.3534 |
| | 82.1 | .106 | 1.1036 | -.0291 | 1.108 | .0459 | -.3178 |
| | 82.1 | .108 | 1.1065 | -.0288 | 1.111 | .0446 | -.3169 |
| | 92.1 | -.052 | 1.1475 | -.0632 | 1.149 | .0099 | -.3497 |
| | 102.1 | -.203 | 1.1615 | -.0902 | 1.178 | -.0452 | -.3777 |
| | | | | M = 1.20 | | | |
| Low-angle sting | -3.1 | -0.066 | 0.2981 | -0.0123 | -0.082 | 0.2941 | -0.3053 |
| | .0 | -.011 | .2914 | .0013 | -.011 | .2914 | -.2889 |
| | .0 | -.020 | .2890 | .0017 | -.020 | .2890 | -.2874 |
| | 4.1 | .080 | .2994 | .0169 | .101 | .2929 | -.3464 |
| | 8.2 | .168 | .3228 | .0317 | .212 | .2955 | -.3675 |
| | 12.3 | .266 | .3641 | .0427 | .337 | .2992 | -.3948 |
| | 16.4 | .350 | .4168 | .0506 | .463 | .2952 | -.4170 |
| | 20.5 | .460 | .4917 | .0562 | .603 | .2995 | -.4638 |
| High-angle adapter | 20.7 | .432 | .4669 | .0610 | .569 | .2840 | -.3381 |
| | 20.7 | .441 | .4716 | .0611 | .579 | .2851 | -.3394 |
| | 30.9 | .542 | .6257 | .0643 | .786 | .2581 | -.5229 |
| | 41.0 | .510 | .7140 | .0581 | .853 | .2045 | -.4049 |
| | 51.5 | .466 | .8506 | .0423 | .956 | .1657 | -.3535 |
| | 51.5 | .466 | .8497 | .0427 | .955 | .1650 | -.3503 |
| | 61.5 | .378 | .9538 | .0215 | 1.019 | .1229 | -.2818 |
| | 71.6 | .267 | 1.0600 | -.0027 | 1.090 | .0824 | -.2636 |
| | 82.1 | .104 | 1.0765 | -.0282 | 1.081 | .0440 | -.2315 |
| | 92.1 | -.052 | 1.1227 | -.0605 | 1.124 | .0101 | -.2635 |
| | 102.2 | -.205 | 1.1470 | -.0877 | 1.164 | -.0412 | -.3061 |

TABLE II.- AERODYNAMIC COEFFICIENTS FOR THE BODY-FIN CONFIGURATION

[$\delta = 0^{\circ}$]

| Support | $\alpha$, deg | $C_L$ | $C_D$ | $C_m$ | $C_N$ | $C_A$ | $C_{p,b}$ |
|---|---|---|---|---|---|---|---|
| | M = 0.40 | | | | | | |
| Low-angle sting | -3.1 | -0.354 | 0.0801 | 0.0598 | -0.358 | 0.0607 | 0.2264 |
| | -3.1 | -.233 | .0805 | .0575 | -.237 | .0679 | .2588 |
| | -.1 | -.236 | .0522 | .0575 | -.237 | .0519 | .2552 |
| | 4.0 | -.052 | .0270 | .0538 | -.050 | .0306 | .2733 |
| | 8.1 | .125 | .0240 | .0505 | .128 | .0062 | .3093 |
| | 12.1 | .282 | .0514 | .0451 | .286 | -.0090 | .2663 |
| | 16.2 | .472 | .0993 | .0248 | .481 | -.0363 | .3131 |
| | 20.3 | .614 | .1565 | .0169 | .630 | -.0658 | .2918 |
| | M = 0.60 | | | | | | |
| Low-angle sting | -3.2 | -0.323 | 0.0850 | 0.0509 | -0.327 | 0.0667 | 0.1626 |
| | -.1 | -.189 | .0570 | .0507 | -.189 | .0567 | .1930 |
| | -.1 | -.193 | .0570 | .0500 | -.193 | .0566 | .1944 |
| | 4.0 | -.034 | .0321 | .0562 | -.032 | .0344 | .2578 |
| | 8.2 | .141 | .0290 | .0529 | .144 | .0087 | .2752 |
| | 12.3 | .262 | .0558 | .0588 | .268 | -.0012 | .2809 |
| | 16.4 | .446 | .1010 | .0416 | .456 | -.0292 | .2882 |
| | 20.5 | .601 | .1568 | .0368 | .617 | -.0639 | .2828 |
| High-angle adapter | 20.7 | .514 | .1560 | .0399 | .536 | -.0357 | .0938 |
| | 20.7 | .511 | .1541 | .0385 | .532 | -.0364 | .0962 |
| | 31.2 | .870 | .3579 | .0265 | .929 | -.1437 | .0195 |
| | 41.2 | .773 | .6453 | -.0319 | 1.007 | -.0233 | -.4228 |
| | 51.2 | .734 | .8348 | -.0924 | 1.110 | -.0485 | -.5224 |
| | 51.2 | .726 | .8324 | -.0941 | 1.104 | -.0444 | -.5199 |
| | 61.3 | .649 | 1.0572 | -.1436 | 1.239 | -.0611 | -.5199 |
| | 71.3 | .537 | 1.2298 | -.1904 | 1.337 | -.1152 | -.4883 |
| | 81.2 | .339 | 1.3595 | -.2270 | 1.395 | -.1271 | -.4582 |
| | 81.2 | .338 | 1.3610 | -.2272 | 1.397 | -.1263 | -.4586 |
| | 91.2 | .149 | 1.4085 | -.2665 | 1.405 | -.1778 | -.4204 |
| | 101.1 | -.030 | 1.4000 | -.3081 | 1.380 | -.2393 | -.4165 |
| | M = 0.80 | | | | | | |
| Low-angle sting | -3.2 | -0.315 | 0.0925 | 0.0501 | -0.320 | 0.0750 | 0.1740 |
| | -.1 | -.166 | .0661 | .0494 | -.167 | .0659 | .1641 |
| | -.1 | -.179 | .0649 | .0499 | -.179 | .0647 | .1712 |
| | 4.1 | .052 | .0573 | .0428 | .056 | .0534 | .1421 |
| | 8.2 | .213 | .0832 | .0476 | .223 | .0521 | .1593 |
| | 12.3 | .338 | .1242 | .0508 | .357 | .0496 | .1127 |
| | 16.3 | .431 | .1829 | .0522 | .465 | .0544 | .0588 |
| | 20.4 | .510 | .2703 | .0425 | .572 | .0758 | .0441 |
| High-angle adapter | 21.2 | .539 | .2538 | .0469 | .594 | .0422 | -.1866 |
| | 31.4 | .601 | .4826 | .0108 | .765 | .0987 | -.4313 |
| | 41.7 | .685 | .7316 | -.0505 | .998 | .0911 | -.5295 |
| | 51.9 | .698 | .9340 | -.1034 | 1.166 | .0273 | -.5140 |
| | 51.9 | .695 | .9333 | -.1034 | 1.163 | .0297 | -.5129 |
| | 62.1 | .655 | 1.1776 | -.1540 | 1.347 | -.0274 | -.4999 |
| | 72.2 | .537 | 1.3680 | -.2008 | 1.467 | -.0926 | -.4837 |
| | 81.4 | .354 | 1.4907 | -.2469 | 1.527 | -.1280 | -.4768 |
| | 81.5 | .352 | 1.4926 | -.2477 | 1.528 | -.1276 | -.4778 |
| | 91.5 | .144 | 1.5640 | -.2914 | 1.560 | -.1843 | -.4721 |
| | 101.3 | -.065 | 1.5702 | -.3325 | 1.553 | -.2445 | -.4756 |
| | M = 0.90 | | | | | | |
| Low-angle sting | -3.1 | -0.109 | 0.1765 | 0.0046 | -0.118 | 0.1704 | -0.2258 |
| | .0 | -.018 | .1723 | .0055 | -.018 | .1723 | -.2344 |
| | .0 | -.017 | .1732 | .0072 | -.017 | .1732 | -.2362 |
| | 4.1 | .089 | .1821 | .0157 | .102 | .1752 | -.2301 |
| | 8.2 | .157 | .1932 | .0327 | .183 | .1690 | -.2152 |
| | 12.2 | .221 | .2235 | .0461 | .263 | .1717 | -.2345 |
| | 16.3 | .255 | .2619 | .0522 | .318 | .1800 | -.2910 |
| | 20.3 | .268 | .3069 | .0540 | .357 | .1951 | -.3554 |
| High-angle adapter | 20.9 | .384 | .3340 | .0558 | .478 | .1749 | -.3949 |
| | 20.9 | .353 | .3256 | .0592 | .445 | .1786 | -.3896 |
| | 31.2 | .502 | .5295 | .0054 | .703 | .1931 | -.5037 |
| | 41.6 | .676 | .7820 | -.0577 | 1.025 | .1361 | -.5371 |
| | 52.3 | .716 | 1.0185 | -.1094 | 1.244 | .0570 | -.5300 |
| | 52.3 | .717 | 1.0198 | -.1101 | 1.246 | .0566 | -.5309 |
| | 62.6 | .688 | 1.2881 | -.1706 | 1.460 | -.0170 | -.5256 |
| | 72.7 | .551 | 1.4746 | -.2180 | 1.572 | -.0871 | -.4972 |
| | 81.3 | .388 | 1.5895 | -.2600 | 1.630 | -.1440 | -.4886 |
| | 81.3 | .383 | 1.5945 | -.2605 | 1.634 | -.1386 | -.4892 |
| | 91.3 | .159 | 1.6673 | -.3051 | 1.663 | -.1977 | -.4605 |
| | 101.3 | -.079 | 1.7010 | -.3482 | 1.684 | -.2559 | -.5045 |
| | M = 0.95 | | | | | | |
| Low-angle sting | -3.1 | -0.096 | 0.2211 | -0.0035 | -0.108 | 0.2156 | -0.2896 |
| | .0 | -.022 | .2147 | .0063 | -.022 | .2147 | -.2937 |
| | .0 | -.016 | .2148 | .0052 | -.016 | .2148 | -.2910 |
| | 4.1 | .077 | .2162 | .0168 | .092 | .2102 | -.2794 |
| | 8.2 | .163 | .2343 | .0302 | .195 | .2088 | -.2694 |
| | 12.3 | .245 | .2662 | .0406 | .296 | .2082 | -.2965 |
| | 16.3 | .292 | .3052 | .0501 | .366 | .2110 | -.3638 |
| | 20.4 | .337 | .3537 | .0461 | .439 | .2143 | -.3902 |
| High-angle adapter | 20.9 | .456 | .3966 | .0427 | .568 | .2075 | -.4568 |
| | 20.9 | .460 | .3975 | .0428 | .572 | .2070 | -.4567 |
| | 31.1 | .541 | .5726 | -.0032 | .759 | .2109 | -.5294 |
| | 41.5 | .738 | .8404 | -.0714 | 1.110 | .1403 | -.5624 |
| | 52.6 | .760 | 1.0932 | -.1226 | 1.330 | .0609 | -.5599 |
| | 52.6 | .762 | 1.0944 | -.1224 | 1.332 | .0606 | -.5613 |
| | 62.8 | .715 | 1.3552 | -.1833 | 1.532 | -.0172 | -.5389 |
| | 73.0 | .570 | 1.5471 | -.2297 | 1.646 | -.0917 | -.5090 |
| | 81.5 | .396 | 1.6316 | -.2659 | 1.672 | -.1485 | -.4794 |
| | 81.5 | .395 | 1.6300 | -.2656 | 1.671 | -.1484 | -.4789 |
| | 91.4 | .157 | 1.7156 | -.3110 | 1.711 | -.1998 | -.4753 |
| | 101.4 | -.081 | 1.7194 | -.3485 | 1.702 | -.2598 | -.4749 |
| | M = 1.00 | | | | | | |
| Low-angle sting | -3.1 | -0.159 | 0.2872 | 0.0282 | -0.174 | 0.2782 | -0.4007 |
| | .0 | -.039 | .2674 | .0175 | -.039 | .2674 | -.3710 |
| | .0 | -.038 | .2671 | .0174 | -.039 | .2671 | -.3700 |
| | 4.1 | .089 | .2692 | .0167 | .108 | .2622 | -.3501 |
| | 8.2 | .225 | .2899 | .0124 | .265 | .2547 | -.3774 |
| | 12.3 | .343 | .3338 | .0174 | .407 | .2527 | -.4179 |
| | 16.4 | .427 | .3836 | .0260 | .518 | .2474 | -.4300 |
| | 20.5 | .506 | .4391 | .0196 | .627 | .2342 | -.3716 |
| High-angle adapter | 20.9 | .562 | .4692 | .0156 | .692 | .2377 | -.4797 |
| | 20.9 | .565 | .4706 | .0160 | .696 | .2378 | -.4815 |
| | 31.1 | .667 | .6596 | -.0216 | .912 | .2195 | -.5968 |
| | 41.4 | .811 | .9050 | -.0871 | 1.207 | .1427 | -.6031 |
| | 52.3 | .815 | 1.1604 | -.1339 | 1.416 | .0657 | -.5861 |
| | 52.3 | .815 | 1.1595 | -.1340 | 1.416 | .0650 | -.5848 |
| | 62.5 | .755 | 1.4203 | -.1909 | 1.609 | -.0138 | -.5437 |
| | 72.6 | .599 | 1.6008 | -.2409 | 1.707 | -.0909 | -.5245 |
| | 81.5 | .411 | 1.6995 | -.2775 | 1.742 | -.1548 | -.4852 |
| | 81.5 | .412 | 1.7001 | -.2779 | 1.742 | -.1556 | -.4849 |
| | 91.5 | .163 | 1.7588 | -.3169 | 1.754 | -.2076 | -.4634 |
| | 101.4 | -.081 | 1.7522 | -.3520 | 1.734 | -.2660 | -.4730 |
| | M = 1.03 | | | | | | |
| Low-angle sting | -3.1 | -0.177 | 0.3049 | 0.0363 | -0.194 | 0.2948 | -0.4157 |
| | .0 | -.052 | .2857 | .0231 | -.052 | .2857 | -.3870 |
| | .0 | -.052 | .2859 | .0231 | -.052 | .2859 | -.3867 |
| | 4.1 | .090 | .2856 | .0153 | .111 | .2784 | -.3707 |
| | 8.2 | .246 | .3092 | .0062 | .288 | .2707 | -.4000 |
| | 12.4 | .371 | .3529 | .0067 | .437 | .2654 | -.4232 |
| | 16.4 | .460 | .4071 | .0140 | .557 | .2601 | -.4153 |
| | 20.5 | .563 | .4729 | .0041 | .693 | .2455 | -.3172 |
| High-angle adapter | 20.9 | .576 | .4793 | .0095 | .709 | .2424 | -.4433 |
| | 20.9 | .578 | .4805 | .0086 | .712 | .2425 | -.4464 |
| | 31.2 | .709 | .6809 | -.0276 | .959 | .2156 | -.5855 |
| | 41.4 | .840 | .9326 | -.0937 | 1.247 | .1433 | -.6069 |
| | 52.4 | .827 | 1.1757 | -.1372 | 1.436 | .0633 | -.5740 |
| | 52.4 | .828 | 1.1760 | -.1378 | 1.437 | .0621 | -.5721 |
| | 62.6 | .765 | 1.4363 | -.1935 | 1.627 | -.0172 | -.5294 |
| | 72.7 | .607 | 1.6258 | -.2457 | 1.733 | -.0950 | -.5059 |
| | 81.4 | .418 | 1.7188 | -.2813 | 1.762 | -.1562 | -.4859 |
| | 81.4 | .419 | 1.7241 | -.2818 | 1.767 | -.1562 | -.4864 |
| | 91.4 | .167 | 1.7627 | -.3173 | 1.758 | -.2089 | -.4606 |
| | 101.3 | -.082 | 1.7819 | -.3564 | 1.763 | -.2688 | -.4741 |
| | M = 1.13 | | | | | | |
| Low-angle sting | -3.1 | -0.168 | 0.2884 | 0.0332 | -0.183 | 0.2789 | -0.2857 |
| | .0 | -.049 | .2693 | .0214 | -.049 | .2693 | -.2569 |
| | .0 | -.054 | .2691 | .0217 | -.055 | .2691 | -.2559 |
| | 4.1 | .081 | .2712 | .0127 | .100 | .2647 | -.2496 |
| | 8.2 | .224 | .2954 | .0047 | .263 | .2605 | -.2771 |
| | 12.3 | .351 | .3396 | .0027 | .416 | .2569 | -.3012 |
| | 16.4 | .452 | .3974 | .0040 | .546 | .2534 | -.2815 |
| | 20.5 | .550 | .4631 | -.0051 | .678 | .2411 | -.1790 |
| High-angle adapter | 20.9 | .536 | .4543 | .0087 | .663 | .2333 | -.3281 |
| | 20.9 | .538 | .4555 | .0077 | .665 | .2336 | -.3290 |
| | 31.2 | .688 | .6556 | -.0307 | .928 | .2042 | -.4443 |
| | 41.5 | .830 | .9198 | -.0943 | 1.231 | .1388 | -.4850 |
| | 52.4 | .807 | 1.1449 | -.1352 | 1.400 | .0581 | -.4455 |
| | 52.5 | .809 | 1.1485 | -.1358 | 1.404 | .0583 | -.4440 |
| | 62.7 | .748 | 1.4038 | -.1901 | 1.590 | -.0200 | -.4092 |
| | 72.8 | .601 | 1.6092 | -.2463 | 1.715 | -.0983 | -.4074 |
| | 81.5 | .413 | 1.7094 | -.2820 | 1.752 | -.1553 | -.3907 |
| | 81.5 | .414 | 1.7151 | -.2809 | 1.758 | -.1554 | -.3921 |
| | 91.4 | .165 | 1.7654 | -.3195 | 1.761 | -.2094 | -.3920 |
| | 101.4 | -.089 | 1.7968 | -.3575 | 1.779 | -.2681 | -.4176 |
| | M = 1.20 | | | | | | |
| Low-angle sting | -3.1 | -0.212 | 0.3359 | 0.0493 | -0.230 | 0.3239 | -0.3849 |
| | .0 | -.077 | .3137 | .0316 | -.077 | .3137 | -.3585 |
| | .0 | -.081 | .3145 | .0316 | -.081 | .3145 | -.3582 |
| | 4.1 | .089 | .3151 | .0131 | .111 | .3079 | -.3486 |
| | 8.2 | .232 | .3408 | .0011 | .279 | .3041 | -.3571 |
| | 12.3 | .372 | .3818 | -.0077 | .445 | .2936 | -.3637 |
| | 16.5 | .520 | .4501 | -.0234 | .626 | .2843 | -.3106 |
| | 20.5 | .589 | .5073 | -.0167 | .729 | .2685 | -.2014 |
| High-angle adapter | 20.8 | .576 | .4975 | -.0152 | .715 | .2601 | -.3385 |
| | 20.9 | .585 | .5011 | -.0137 | .725 | .2601 | -.3396 |
| | 31.1 | .728 | .6954 | -.0395 | .983 | .2190 | -.4694 |
| | 41.3 | .794 | .9033 | -.0816 | 1.192 | .1545 | -.4482 |
| | 52.5 | .775 | 1.1186 | -.1267 | 1.359 | .0676 | -.3765 |
| | 52.5 | .776 | 1.1156 | -.1267 | 1.357 | .0651 | -.3762 |
| | 62.7 | .723 | 1.3637 | -.1837 | 1.543 | -.0166 | -.3144 |
| | 72.8 | .587 | 1.5726 | -.2396 | 1.676 | -.0951 | -.3119 |
| | 81.5 | .403 | 1.6653 | -.2759 | 1.707 | -.1518 | -.2977 |
| | 91.4 | .161 | 1.7199 | -.3132 | 1.715 | -.2045 | -.3023 |
| | 101.4 | -.086 | 1.7508 | -.3528 | 1.733 | -.2619 | -.3399 |

TABLE III.- AERODYNAMIC COEFFICIENTS FOR THE BODY-FIN CONFIGURATION

[$\delta$ = - 20°]

| | α, deg | $C_L$ | $C_D$ | $C_m$ | $C_N$ | $C_A$ | $C_{p,b}$ |
|---|---|---|---|---|---|---|---|
| | | | | M = 0.40 | | | |
| Low-angle sting | -3.6 | -0.502 | 0.1652 | 0.1008 | -0.512 | 0.1332 | 0.1437 |
| | -.1 | -.425 | .1305 | .1205 | -.425 | .1297 | .1937 |
| | 3.9 | -.310 | .0962 | .1360 | -.302 | .1173 | .2299 |
| | 8.0 | -.190 | .0608 | .1470 | -.179 | .0866 | .2551 |
| | 12.1 | -.021 | .0428 | .1426 | -.012 | .0462 | .2873 |
| | 16.1 | .178 | .0470 | .1298 | .184 | -.0042 | .2552 |
| | 20.2 | .364 | .0785 | .1143 | .369 | -.0522 | .1834 |
| | | | | M = 0.60 | | | |
| Low-angle sting | -3.8 | -0.492 | 0.1698 | 0.0994 | -0.502 | 0.1372 | 0.1113 |
| | -.2 | -.414 | .1354 | .1204 | -.414 | .1339 | .1717 |
| | 3.9 | -.300 | .1007 | .1406 | -.293 | .1209 | .2116 |
| | 8.0 | -.188 | .0679 | .1570 | -.176 | .0934 | ..2459 |
| | 12.2 | .004 | .0436 | .1475 | .013 | .0418 | .2497 |
| | 16.3 | .148 | .0476 | .1487 | .155 | .0044 | .2369 |
| | 20.4 | .350 | .0839 | .1332 | .357 | -.0435 | .1731 |
| High-angle adapter | 20.6 | .328 | .0988 | .1219 | .342 | -.0229 | .1138 |
| | 20.6 | .330 | .1002 | .1212 | .345 | -.0224 | .1162 |
| | 31.1 | .741 | .2539 | .0948 | .766 | -.1650 | .0654 |
| | 41.1 | .735 | .5375 | .0226 | .907 | -.0788 | -.4247 |
| | 51.1 | .619 | .6927 | .0332 | .928 | -.0460 | -.4738 |
| | 51.1 | .626 | .6951 | .0331 | .934 | -.0502 | -.4726 |
| | 61.1 | .563 | .8808 | .0872 | 1.043 | -.0680 | -.4920 |
| | 71.2 | .502 | 1.0793 | .1416 | 1.183 | -.1278 | -.4920 |
| | | | | M = 0.80 | | | |
| Low-angle sting | -3.7 | -0.507 | 0.1781 | 0.1054 | -0.518 | 0.1451 | 0.0956 |
| | -.1 | -.394 | .1425 | .1242 | -.394 | .1415 | .0808 |
| | 4.0 | -.235 | .1101 | .1381 | -.227 | .1261 | .0661 |
| | 8.1 | -.049 | .0981 | .1439 | -.035 | .1040 | .0319 |
| | 12.2 | .166 | .1199 | .1294 | .187 | .0822 | .0025 |
| | 16.3 | .363 | .1821 | .0858 | .400 | .0728 | -.1426 |
| | 20.3 | .314 | .2526 | .0884 | .382 | .1282 | -.2970 |
| High-angle adapter | 21.0 | .362 | .2050 | .1114 | .411 | .0617 | -.1262 |
| | 21.0 | .365 | .2076 | .1112 | .415 | .0629 | -.1335 |
| | 31.3 | .468 | .3904 | .0846 | .602 | .0909 | -.3939 |
| | 41.4 | .461 | .5505 | .0356 | .709 | .1089 | -.4371 |
| | 51.6 | .524 | .7614 | .0203 | .922 | .0619 | -.4935 |
| | 51.6 | .525 | .7634 | .0204 | .924 | .0624 | -.4943 |
| | 61.8 | .530 | .9753 | .0818 | 1.110 | -.0069 | -.4821 |
| | 72.0 | .475 | 1.1801 | .1414 | 1.269 | -.0862 | -.4715 |
| | | | | M = 0.90 | | | |
| Low-angle sting | -3.7 | -0.414 | 0.2601 | 0.1100 | -0.430 | 0.2332 | -0.1806 |
| | -.1 | -.252 | .2186 | .0985 | -.252 | .2182 | -.2021 |
| | 4.0 | -.055 | .1946 | .0841 | -.041 | .1980 | -.2387 |
| | 8.2 | .148 | .1925 | .0560 | .174 | .1695 | -.2817 |
| | 12.2 | .218 | .2149 | .0578 | .258 | .1639 | -.2471 |
| | 16.3 | .282 | .2536 | .0576 | .342 | .1644 | -.2684 |
| | 20.3 | .279 | .2943 | .0583 | .363 | .1794 | -.2891 |
| High-angle adapter | 21.0 | .391 | .3065 | .0745 | .475 | .1463 | -.4077 |
| | 21.0 | .393 | .3073 | .0743 | .477 | .1465 | -.4096 |
| | 31.2 | .464 | .4688 | .0637 | .640 | .1603 | -.4425 |
| | 41.4 | .468 | .6264 | .0350 | .765 | .1609 | -.4633 |
| | 51.9 | .511 | .8103 | .0227 | .953 | .0976 | -.4797 |
| | 51.9 | .509 | .8074 | .0222 | .949 | .0976 | -.4789 |
| | 62.2 | .549 | 1.0564 | .0870 | 1.190 | .0067 | -.4875 |
| | 72.4 | .488 | 1.2730 | .1520 | 1.361 | -.0802 | -.4908 |
| | | | | M = 0.95 | | | |
| Low-angle sting | -3.7 | -0.389 | 0.3017 | 0.1093 | -0.408 | 0.2763 | -0.2796 |
| | -.1 | -.188 | .2570 | .0816 | -.188 | .2568 | -.2827 |
| | 4.1 | .006 | .2405 | .0630 | .023 | .2395 | -.3528 |
| | 8.2 | .196 | .2417 | .0405 | .228 | .2114 | -.3607 |
| | 12.3 | .244 | .2562 | .0495 | .293 | .1985 | -.3207 |
| | 16.3 | .317 | .2981 | .0511 | .388 | .1971 | -.3360 |
| | 20.4 | .327 | .3384 | .0544 | .424 | .2035 | -.3231 |
| High-angle adapter | 20.9 | .422 | .3707 | .0645 | .527 | .1960 | -.4656 |
| | 20.9 | .420 | .3676 | .0638 | .524 | .1937 | -.4633 |
| | 31.1 | .456 | .5190 | .0652 | .658 | .2094 | -.4638 |
| | 41.2 | .447 | .6555 | .0244 | .768 | .1998 | -.4585 |
| | 52.2 | .556 | .8863 | .0349 | 1.041 | .1046 | -.5085 |
| | 52.2 | .558 | .8914 | .0343 | 1.046 | .1057 | -.5112 |
| | 62.5 | .583 | 1.1346 | .0989 | 1.276 | .0062 | -.5124 |
| | 72.7 | .512 | 1.3487 | .1637 | 1.440 | -.0877 | -.5073 |
| | | | | M = 1.00 | | | |
| Low-angle sting | -3.7 | -0.492 | 0.3882 | 0.1539 | -0.516 | 0.3555 | -0.3162 |
| | -.1 | -.305 | .3450 | .1350 | -.306 | .3444 | -.3678 |
| | 4.1 | -.092 | .3173 | .1094 | -.070 | .3230 | -.4114 |
| | 8.2 | .143 | .3065 | .0660 | .186 | .2829 | -.4506 |
| | 12.3 | .275 | .3164 | .0505 | .336 | .2507 | -.4094 |
| | 16.4 | .374 | .3638 | .0504 | .461 | .2435 | -.4160 |
| | 20.5 | .454 | .4222 | .0496 | .573 | .2366 | -.4399 |
| High-angle adapter | 20.8 | .493 | .4482 | .0590 | .620 | .2439 | -.4787 |
| | 20.8 | .500 | .4513 | .0578 | .627 | .2442 | -.4821 |
| | 30.9 | .471 | .5642 | .0472 | .694 | .2427 | -.5268 |
| | 41.1 | .549 | .7399 | .0023 | .900 | .1972 | -.5187 |
| | 52.3 | .644 | 1.0052 | .0486 | 1.189 | .1053 | -.5837 |
| | 52.3 | .643 | 1.0039 | .0479 | 1.187 | .1054 | -.5839 |
| | 62.5 | .632 | 1.2177 | .1131 | 1.372 | .0019 | -.5514 |
| | 72.6 | .544 | 1.4228 | .1770 | 1.520 | -.0942 | -.5317 |
| | | | | M = 1.03 | | | |
| Low-angle sting | -3.7 | -0.506 | 0.4020 | 0.1613 | -0.531 | 0.3684 | -0.3234 |
| | -3.7 | -.506 | .4016 | .1608 | -.531 | .3682 | -.3230 |
| | -3.7 | -.505 | .4027 | .1614 | -.530 | .3694 | -.3225 |
| | -.1 | -.334 | .3630 | .1458 | -.335 | .3624 | -.3733 |
| | -.1 | -.340 | .3660 | .1489 | -.340 | .3654 | -.3718 |
| | 4.0 | -.121 | .3326 | .1179 | -.097 | .3402 | -.4173 |
| | 8.2 | .134 | .3180 | .0686 | .178 | .2957 | -.4296 |
| | 12.3 | .276 | .3275 | .0477 | .340 | .2612 | -.4272 |
| | 16.4 | .380 | .2767 | .0472 | .471 | .2542 | -.4314 |
| | 20.5 | .481 | .4447 | .0443 | .606 | .2485 | -.4743 |
| High-angle adapter | 20.8 | .498 | .4547 | .0554 | .628 | .2476 | -.4493 |
| | 20.9 | .503 | .4575 | .0545 | .633 | .2484 | -.4501 |
| | 31.0 | .536 | .6048 | .0360 | .771 | .2428 | -.5607 |
| | 41.2 | .638 | .8063 | .0136 | 1.011 | .1863 | -.5730 |
| | 52.1 | .665 | 1.0233 | .0540 | 1.216 | .1030 | -.5806 |
| | 52.1 | .666 | 1.0239 | .0537 | 1.217 | .1030 | -.5825 |
| | 62.3 | .651 | 1.2438 | .1180 | 1.404 | .0011 | -.5511 |
| | 72.5 | .558 | 1.4539 | .1825 | 1.555 | -.0942 | -.5314 |
| | | | | M = 1.13 | | | |
| Low-angle sting | -3.7 | -0.456 | 0.3754 | 0.1462 | -0.479 | 0.3454 | -0.1986 |
| | -.1 | -.294 | .3369 | .1312 | -.295 | .3364 | -.2498 |
| | 4.0 | -.108 | .3108 | .1074 | -.086 | .3177 | -.2795 |
| | 8.2 | .116 | .2998 | .0657 | .157 | .2802 | -.2971 |
| | 12.3 | .254 | .3112 | .0459 | .315 | .2500 | -.3006 |
| | 16.4 | .361 | .3627 | .0433 | .448 | .2463 | -.3088 |
| | 20.5 | .474 | .4355 | .0376 | .596 | .2422 | -.3696 |
| High-angle adapter | 20.8 | .468 | .4318 | .0490 | .591 | .2377 | -.3309 |
| | 20.8 | .472 | .4338 | .0479 | .595 | .2384 | -.3326 |
| | 31.0 | .561 | .5913 | .0237 | .785 | .2187 | -.4416 |
| | 41.2 | .668 | .8077 | .0245 | 1.034 | .1685 | -.4738 |
| | 52.2 | .665 | 1.0106 | .0599 | 1.206 | .0932 | -.4535 |
| | 52.3 | .665 | 1.0116 | .0587 | 1.207 | .0937 | -.4538 |
| | 62.5 | .641 | 1.2246 | .1194 | 1.382 | -.0021 | -.4288 |
| | 72.6 | .553 | 1.4379 | .1833 | 1.537 | -.0972 | -.4223 |
| | | | | M = 1.20 | | | |
| Low-angle sting | -3.7 | -0.481 | 0.4232 | 0.1568 | -0.507 | 0.3914 | -0.3228 |
| | -.1 | -.333 | .3866 | .1420 | -.334 | .3859 | -.3401 |
| | 4.0 | -.133 | .3586 | .1108 | -.107 | .3670 | -.3632 |
| | 8.2 | .060 | .3516 | .0831 | .110 | .3394 | -.3920 |
| | 12.3 | .248 | .3748 | .0557 | .322 | .3134 | -.4131 |
| | 16.4 | .389 | .4122 | .0372 | .489 | .2856 | -.4067 |
| | 20.5 | .520 | .4866 | .0244 | .658 | .2734 | -.4394 |
| High-angle adapter | 20.7 | .489 | .4692 | .0324 | .623 | .2658 | -.3420 |
| | 20.7 | .494 | .4715 | .0326 | .629 | .2658 | -.3429 |
| | 31.0 | .656 | .6636 | .0097 | .904 | .2309 | -.4961 |
| | 41.1 | .637 | .7894 | .0153 | .999 | .1766 | -.4243 |
| | 52.3 | .636 | .9855 | .0536 | 1.168 | .1003 | -.3892 |
| | 52.3 | .634 | .9841 | .0515 | 1.166 | .1016 | -.3890 |
| | 62.5 | .605 | 1.1773 | .1081 | 1.324 | .0082 | -.3405 |
| | 72.6 | .535 | 1.4005 | .1763 | 1.496 | -.0918 | -.3368 |

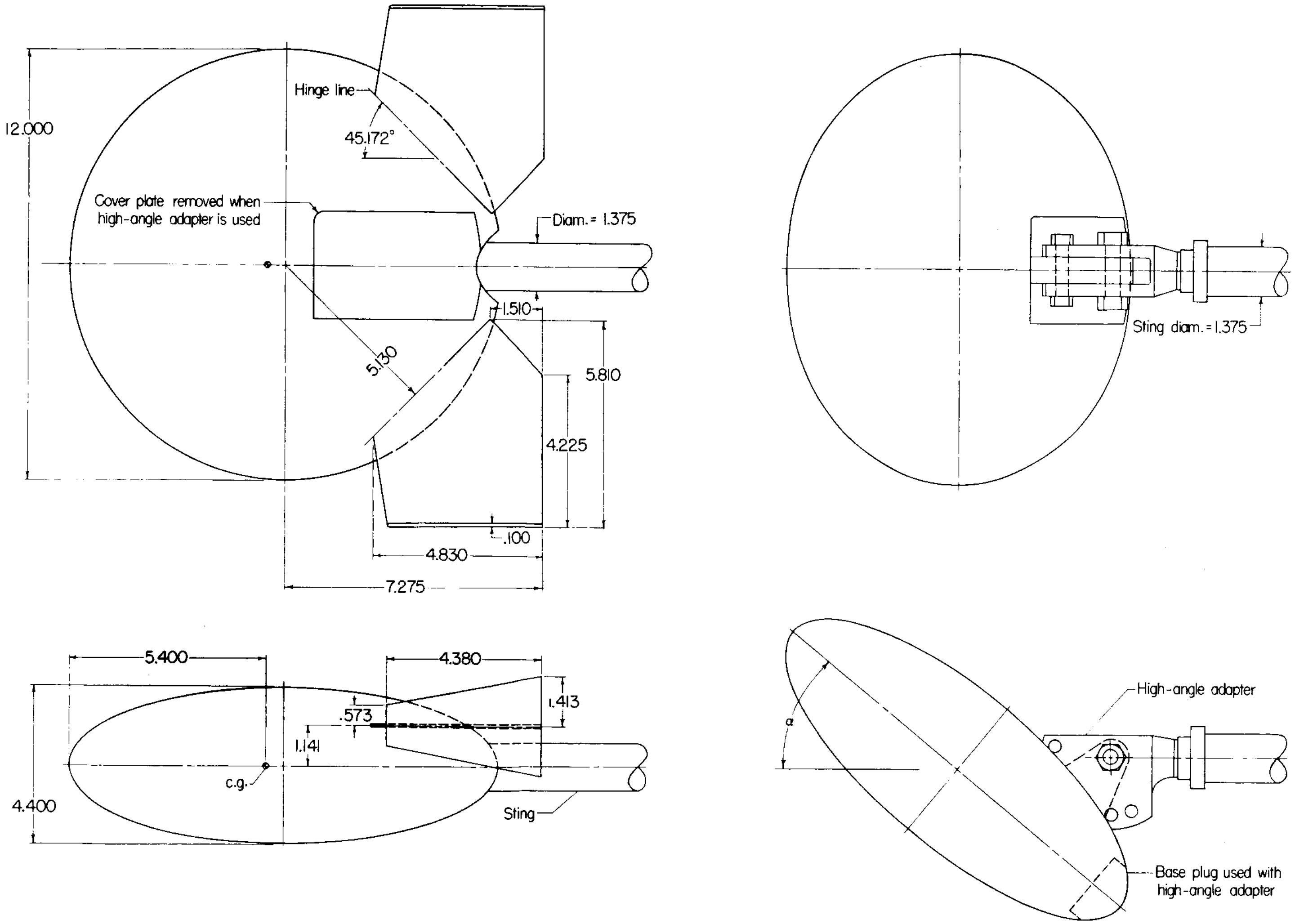


(a) Body-fin model on low-angle sting.

(b) Body-alone model on high-angle adapter.

Figure 1.- Model details showing design dimensions. All dimensions are in inches unless otherwise noted.

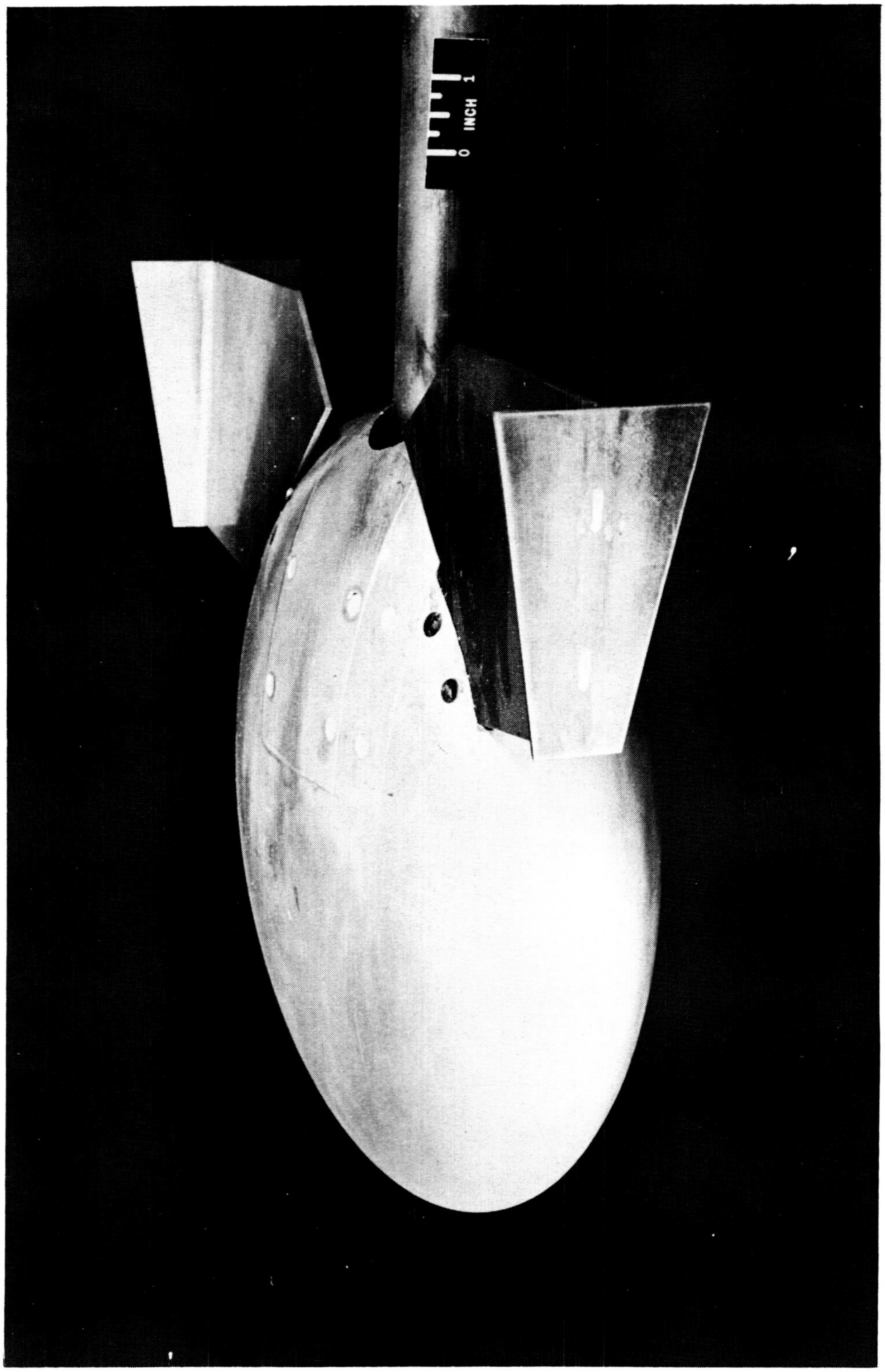


L-60-1632

(a) Body-fin model on low-angle sting

Figure 2.- Photographs of models.

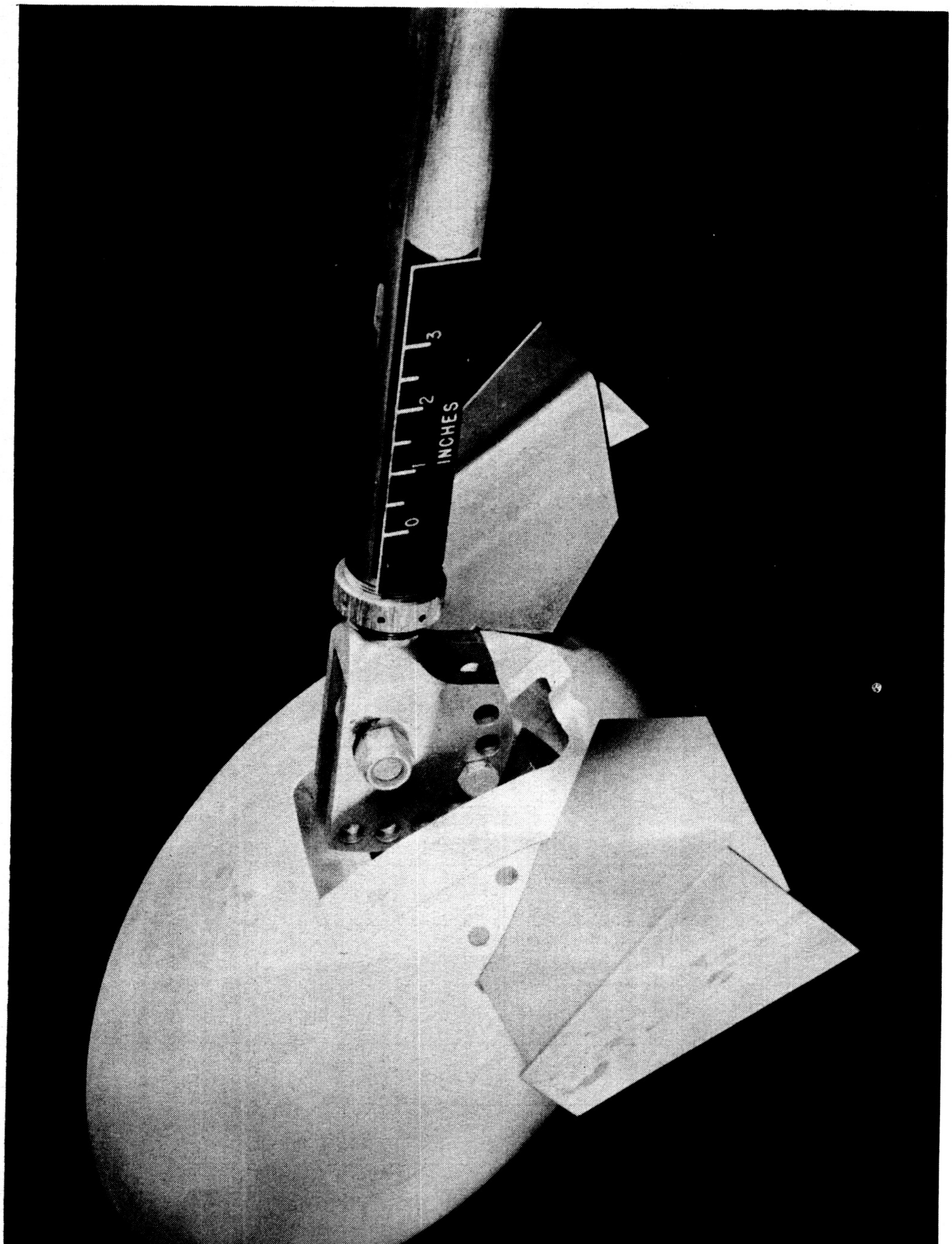


L-60-3172

(b) Body-fin model on high-angle adapter.

Figure 2.- Concluded.

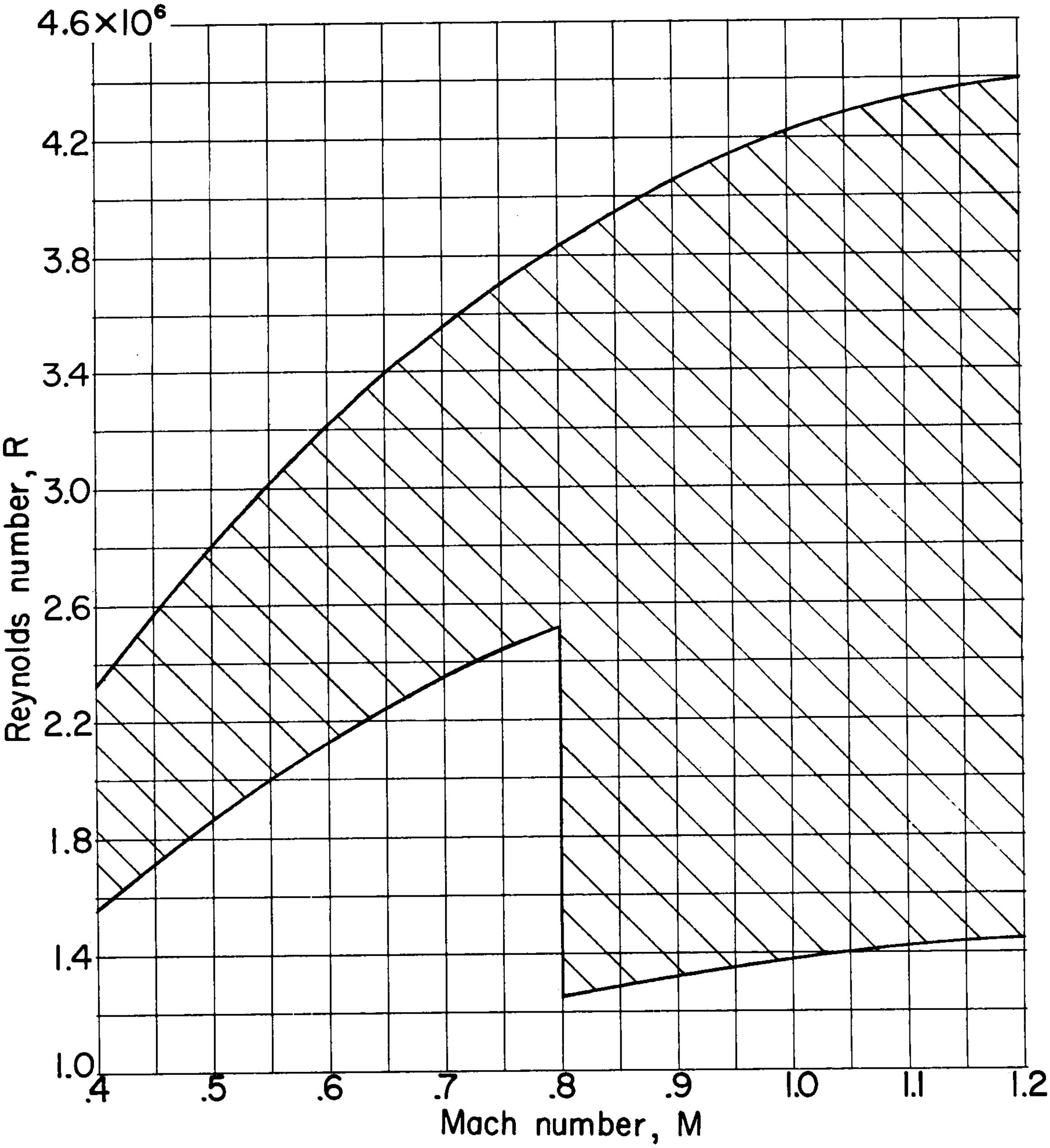


Figure 3.- Variation of Reynolds number range with Mach number. Reynolds number based on body length.

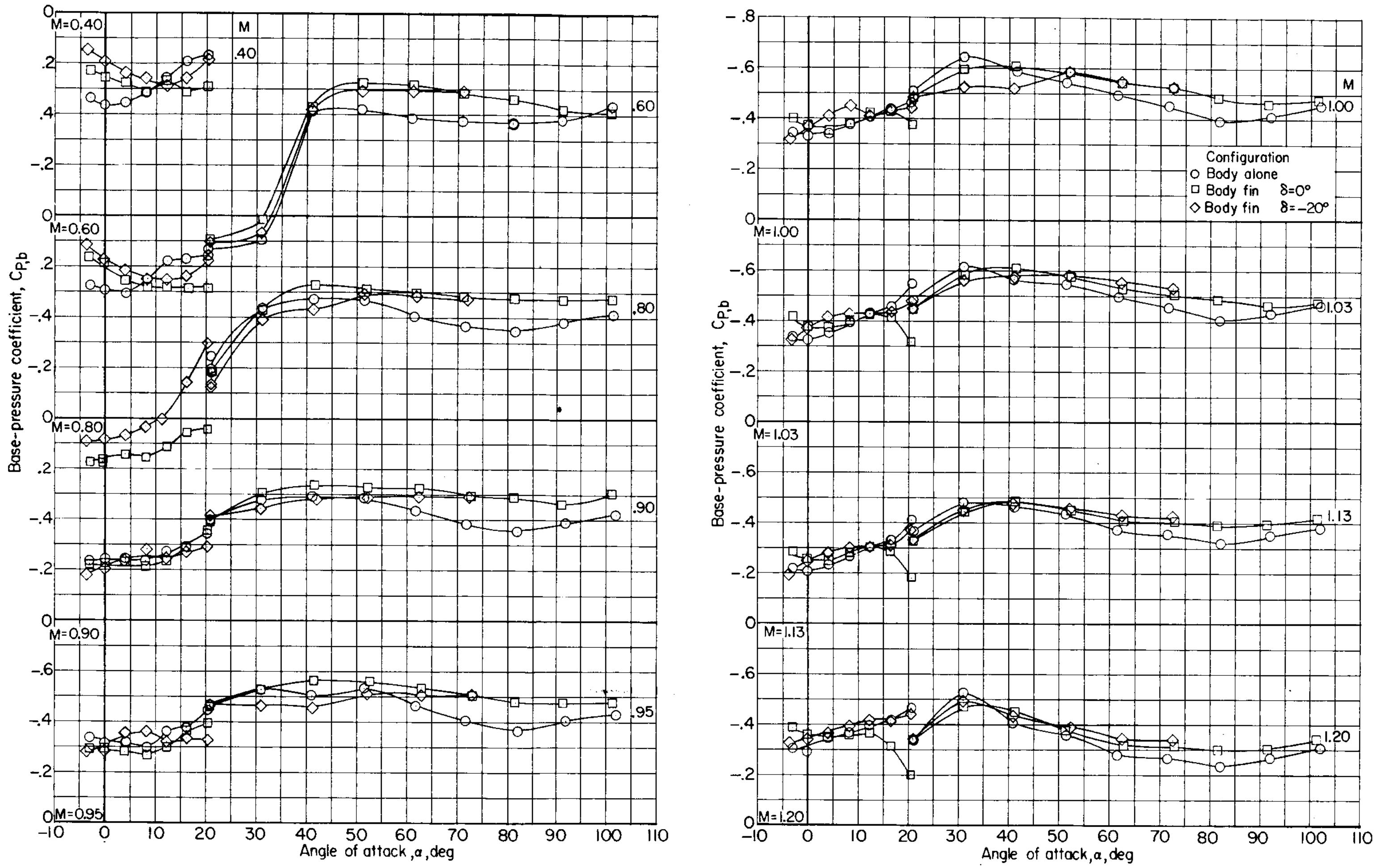


Figure 4.- Base-pressure characteristics of body-alone and body-fin configurations.

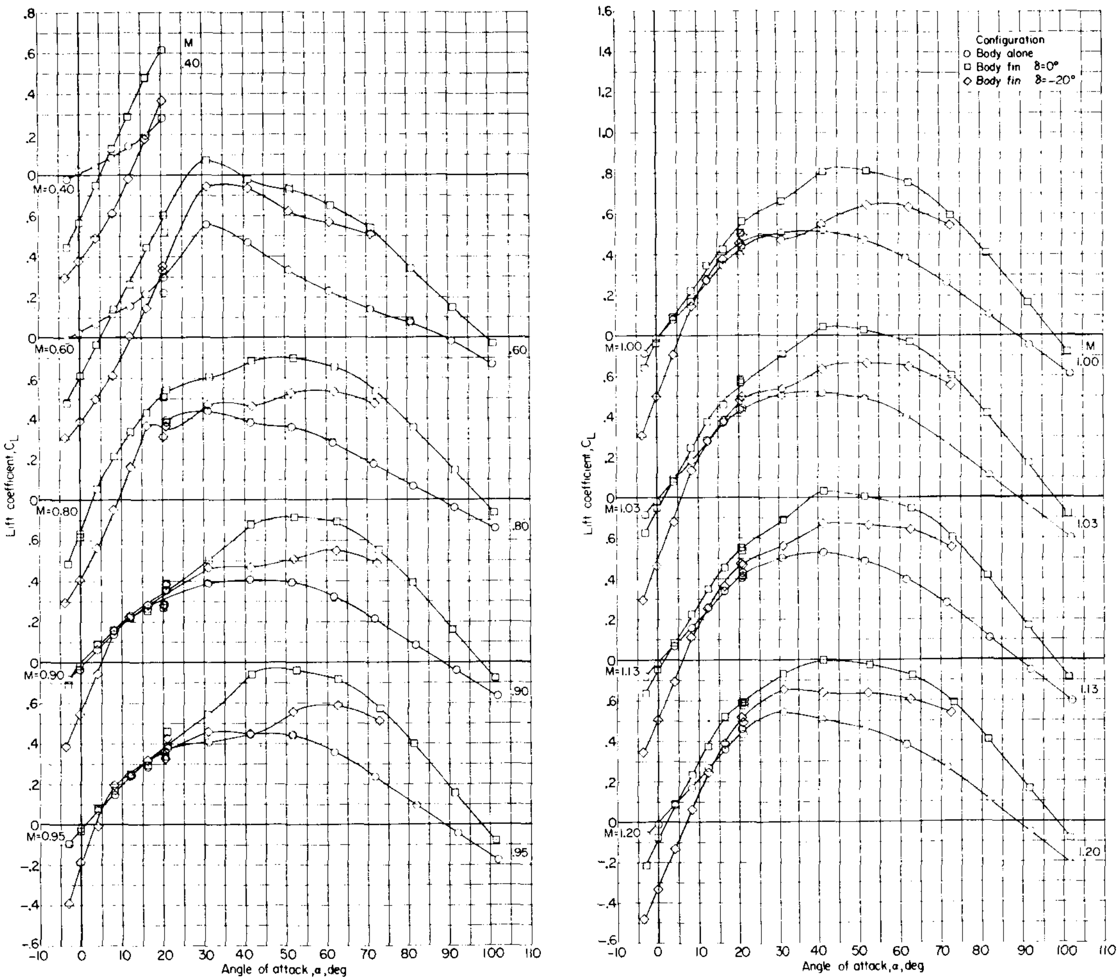


(a) Lift characteristics.

Figure 5.- Aerodynamic characteristics of body-alone and body-fin configurations.

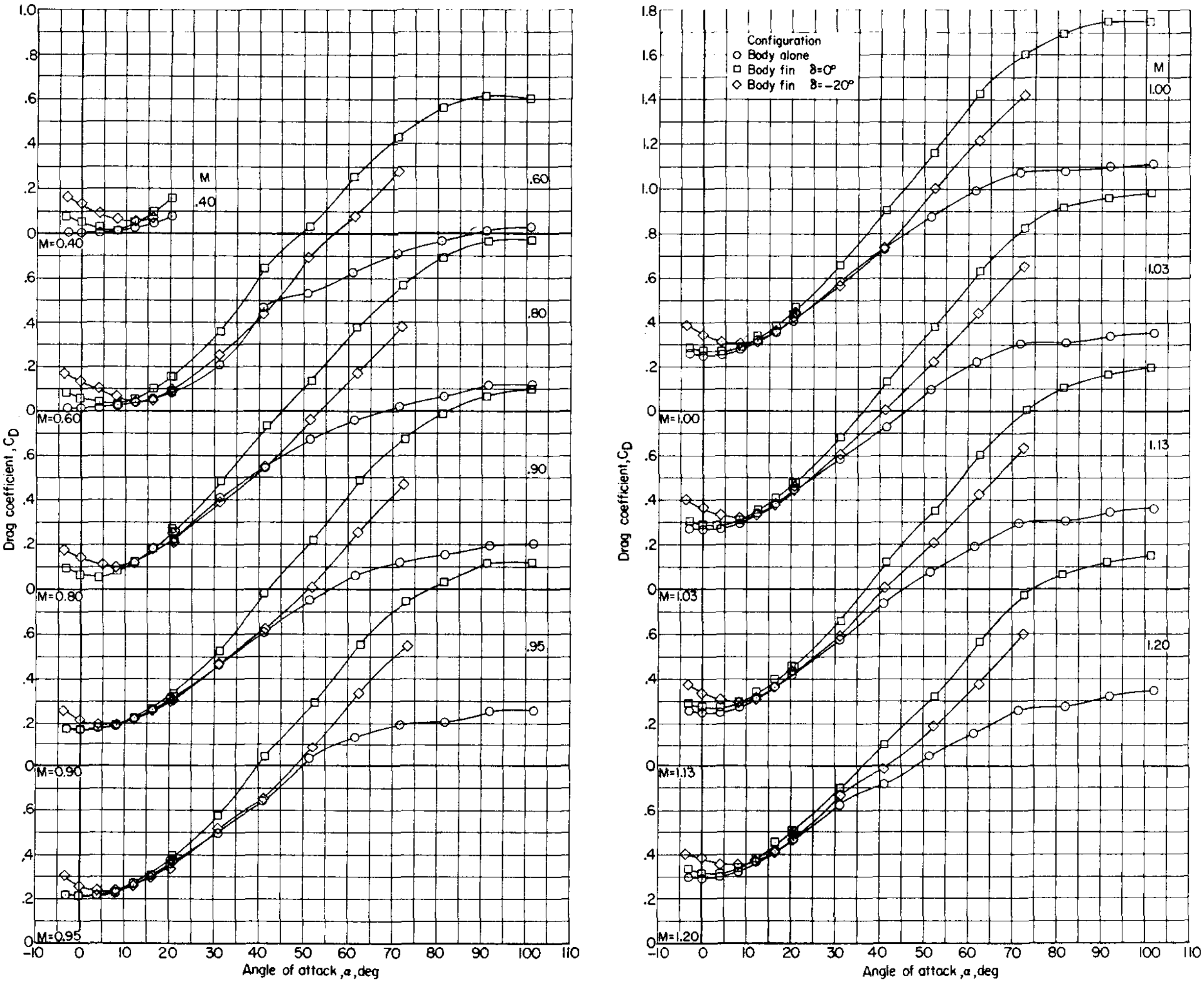


(b) Drag characteristics.

Figure 5.- Continued.

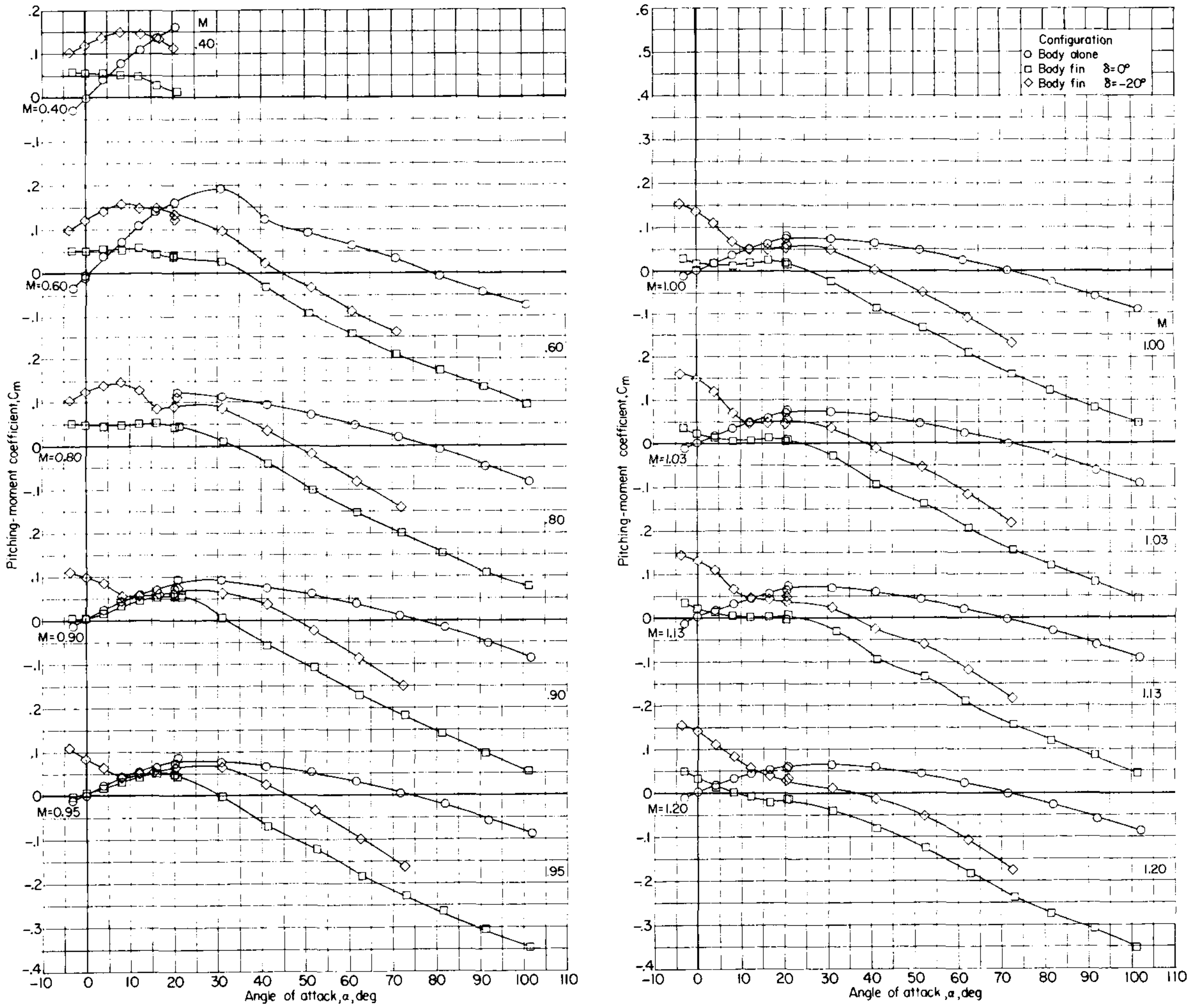


(c) Pitching-moment characteristics.

Figure 5.- Continued.

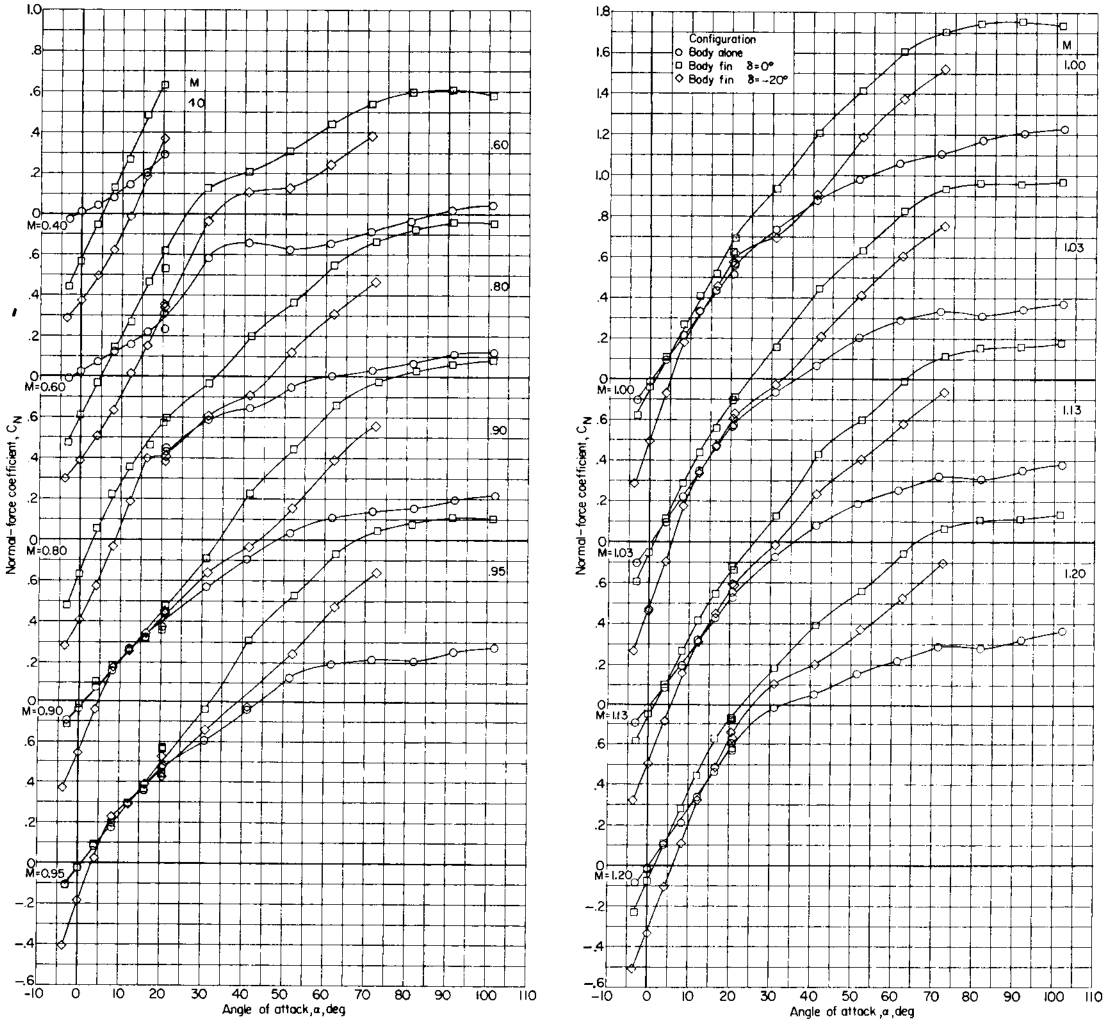


(d) Normal-force characteristics.

Figure 5.- Continued.

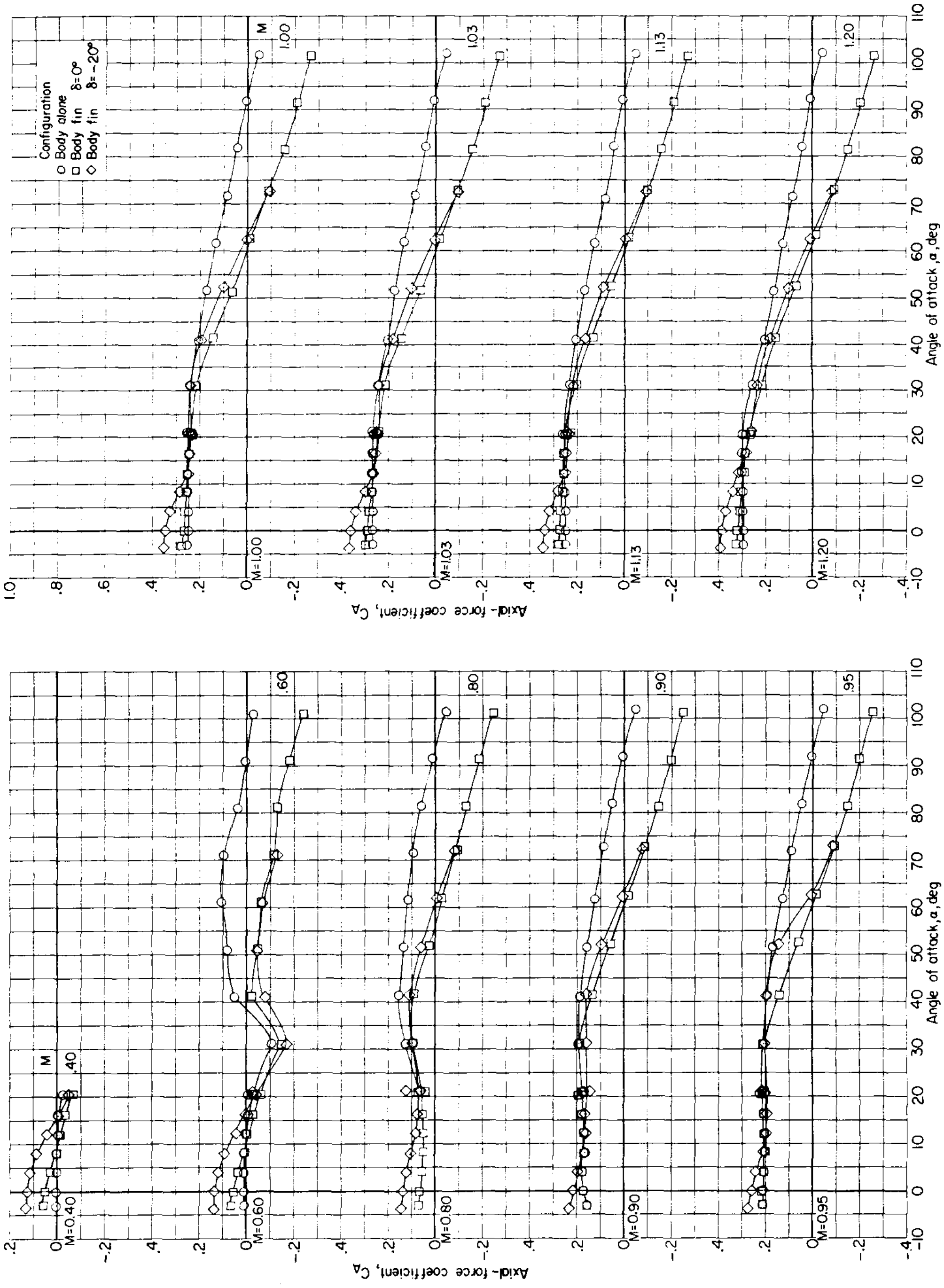


(e) Axial-force characteristics.

Figure 5.- Concluded.

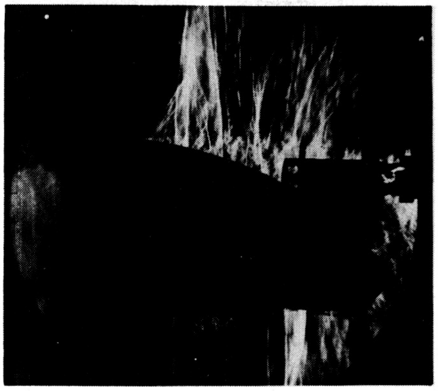

M=0.80

M=0.95

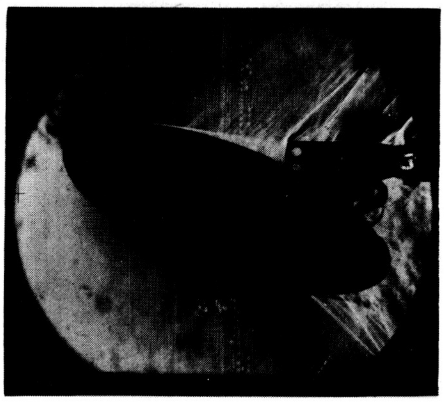

M=1.00

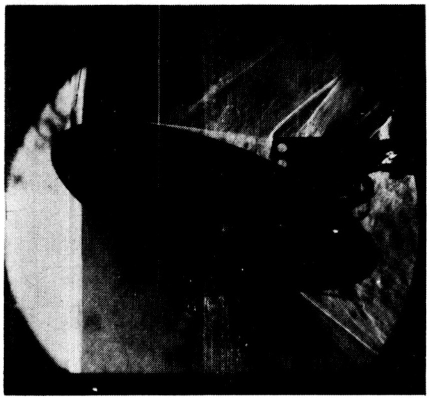

M=1.13

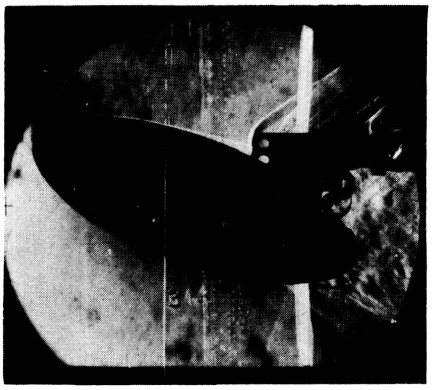

M=1.20

L-60-5547

Figure 6.- Schlieren photographs of the body-alone configuration. $\alpha \approx 20^{\circ}$.

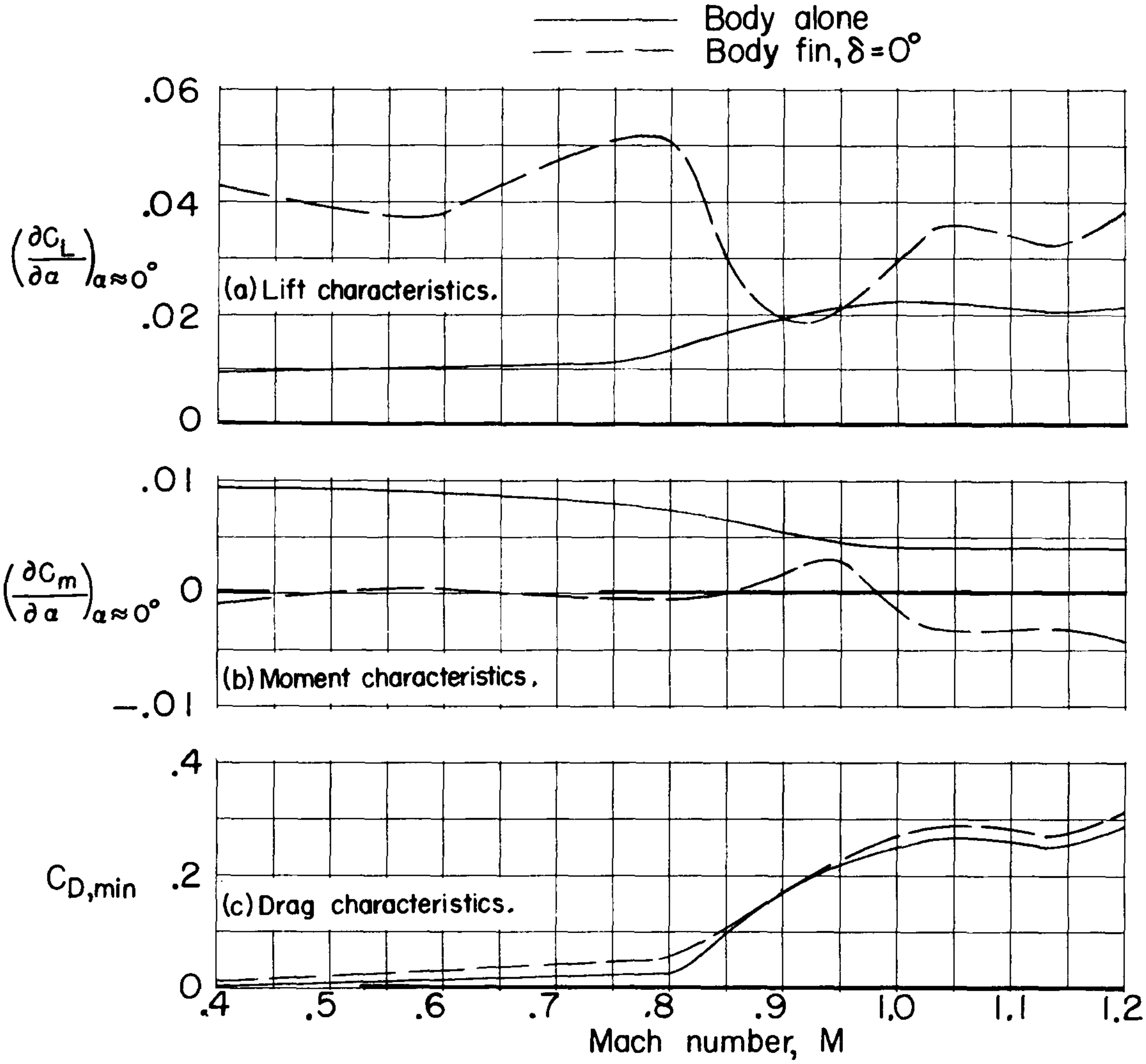


Figure 7.- Summary of the longitudinal aerodynamic parameters at low angles of attack for the body-alone and body-fin, $\delta = 0^{\circ}$ configurations.

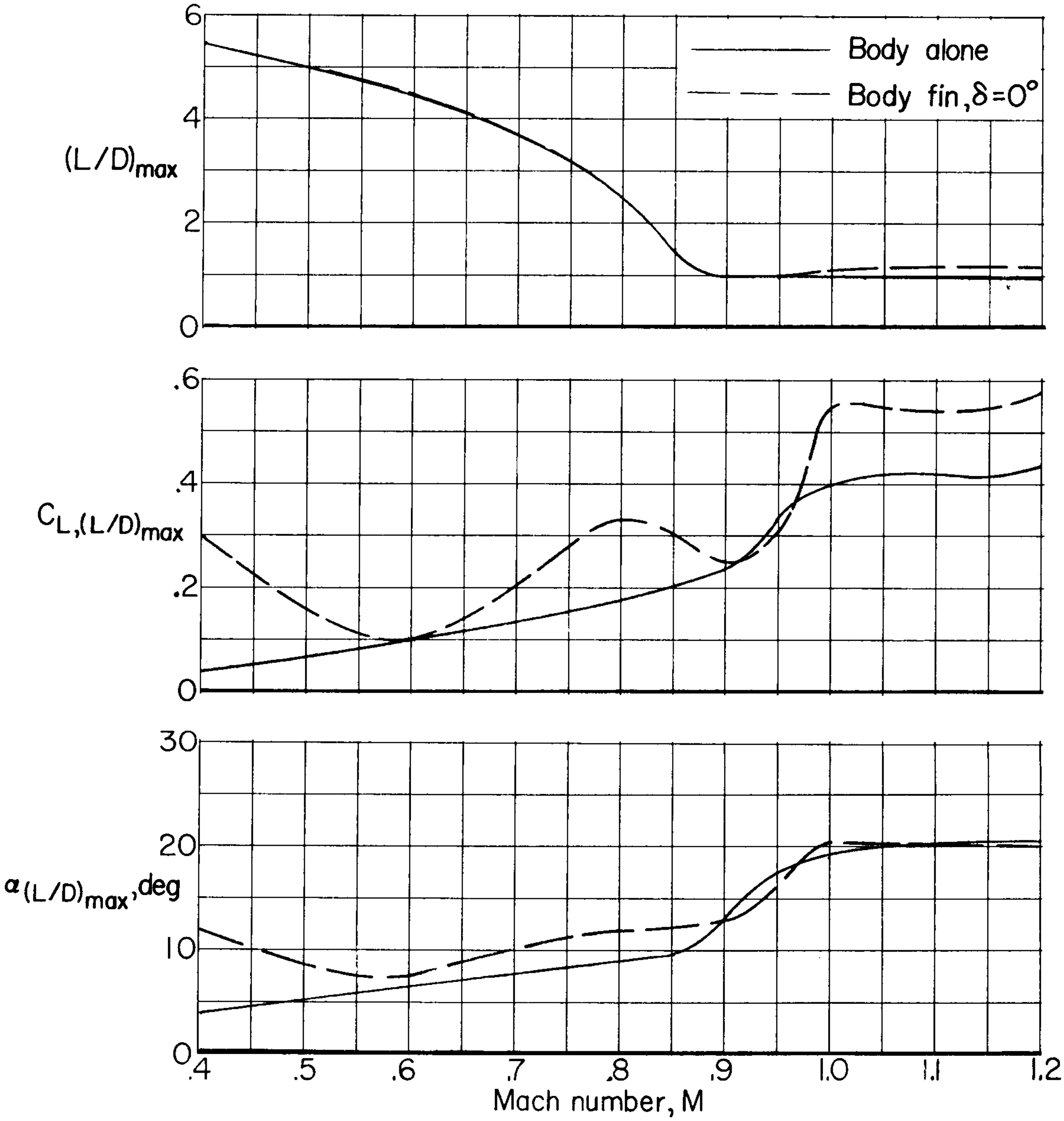


Figure 8.- Summary of maximum lift-drag-ratio characteristics for the body-alone and body-fin, $\delta = 0^{\circ}$ configurations.

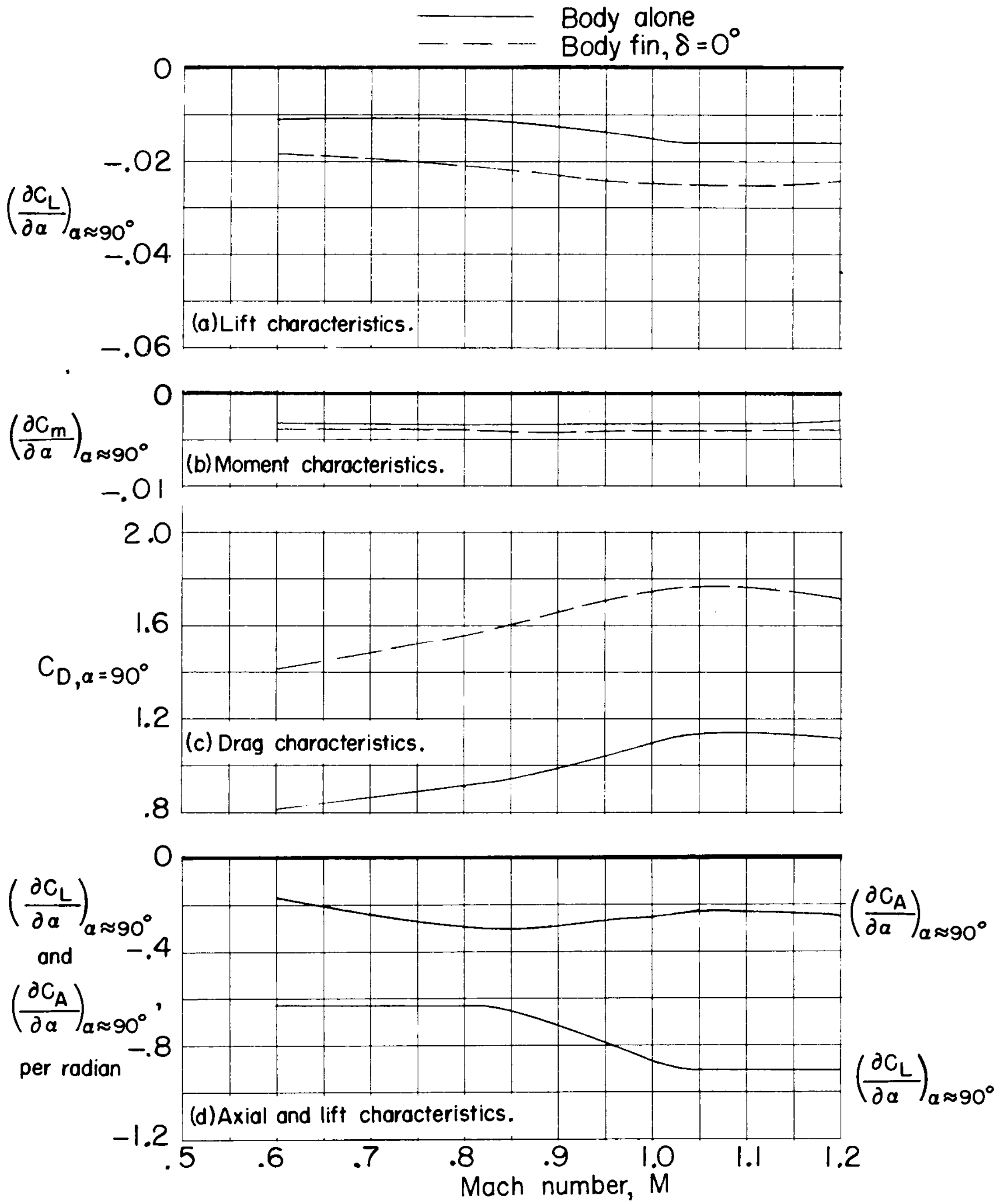


Figure 9.- Summary of the longitudinal aerodynamic parameters at an angle of attack of 90° for the body-alone and body-fin, δ = 0° configurations.

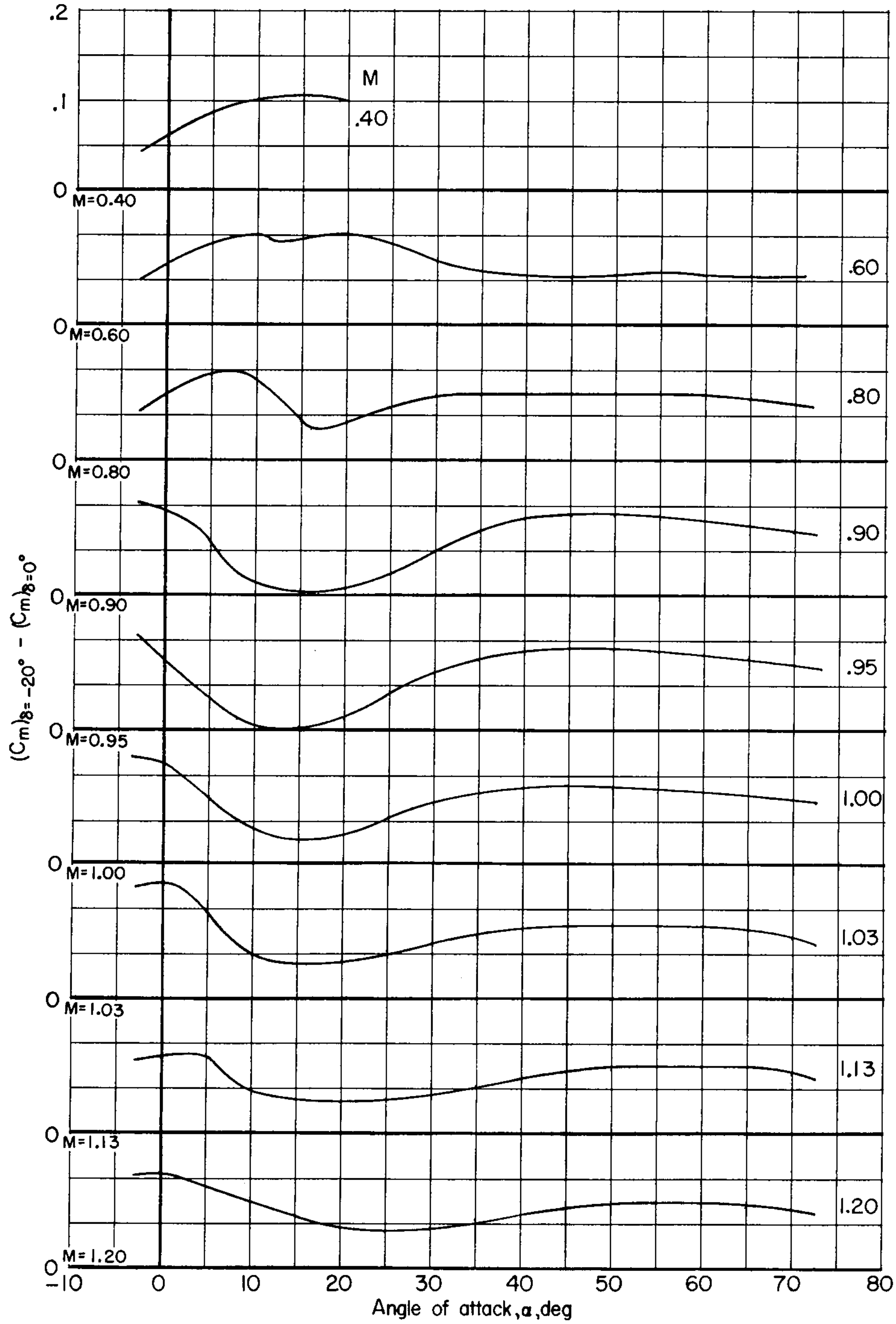


Figure 10.- Effects of a fin deflection of -20° on the pitching-moment characteristics.